Det Kgl. Danske Videnskabernes Selskab.
Mathematisk-fysiske Meddelelser. **XVII**, 11.

ON THE THEORY OF THE EFFECTS OF THE PHOTON COMPONENT IN COINCIDENCE EXPERIMENTS ON COSMIC RAYS

BY

NIELS ARLEY AND BODIL ERIKSEN

KØBENHAVN
EJNAR MUNKSGAARD
1940

TABLE OF CONTENTS

Printed in Denmark.
Bianco Lunos Bogtrykkeri A/S.

INTRODUCTION

In a previous paper[1] one of us has discussed the secondary phenomena produced by the electrons[2] in the soft component of the cosmic radiation. Until now only this part of the soft component has been investigated in detail experimentally as well as theoretically in spite of the fact that the photon part is quite as important. This lack is due partly to the experimental difficulties in isolating the effects of the photons, and partly to the fact that the photons and electrons enter almost symmetrically into the cascade theory, so that their secondary effects are nearly identical, at any rate for large thicknesses of material. For small layers the curves are, however, rather different and for the discussion of the beginning of the coincidence curves it is therefore necessary also to work out the photon curves. Furthermore, for the problem of the existence of neutral mesons[3] it is important to have detailed knowledge of the photon part.

It is the purpose of this paper to discuss the photon part of the soft component in a way analogous to the discussion of the electron part given in A.

[1] ARLEY (1938). In the following quoted as A.

[2] By electrons we shall understand in the following both negatively and positively charged particles, unless otherwise stated.

[3] See e.g. ARLEY and HEITLER (1938); KEMMER (1938); MØLLER (1938). Cf. also the discussion in § 6.

1. Number of electrons and photons above the critical energy.

Let us consider a photon with energy k_0 falling on a layer of material with thickness l expressed in shower-units[1]. By cascade multiplication this photon will give rise to a shower of electrons and photons. We shall now work out the average number of these particles emerging with energies above E or k, respectively, as functions of k_0, l, and E or k, respectively. These functions we deduce in the same way that the corresponding ones for electron-initiated showers were deduced by B & H. For the average number $h(l,k)\,dk$ of photons emerging from a thickness l with energies between k and $k+dk$, we therefore have their equation (16)

$$h(l,k)\,dk = \left[\frac{\log 2}{k}\, e^{-\alpha l}\int_0^l e^{\alpha l'}\left\{f_+(l',k)+f_-(l',k)\right\}dl' + \right. \\ \left. + h(0,k)\, e^{-\alpha l}\right] dk. \qquad (1)$$

Here α is a constant equal to 0.6, $f_+(l',k)$ and $f_-(l',k)$ the average number of positive and negative electrons, respectively, which at the point l' below the surface have energies above k, and $h(0,k)\,dk$ the energy distribution of photons which fall on the surface. Since we have only one incident photon with energy k_0, we have

$$h(0,k)\,dk = \delta\left(\frac{k_0-k}{k_0}\right)\frac{dk}{k_0}; \quad \int_0^\infty h(0,k)\,dk = 1 \qquad (2)$$

(where $\delta(x)$ is the Dirac δ-function), and

[1] BHABHA and HEITLER (1937) (in the following quoted as B & H) and A. Cf. also CARLSON and OPPENHEIMER (1937).

$$f_-(0,k) = f_+(0,k) = 0 \tag{3}$$

so that we have

$$f_-(l,k) = f_+(l,k) = f(l,k) \tag{4}$$

where $f(l,k)$ is the average number of negative *or* positive electrons. Introducing the logarithmic variables

$$y = \log \frac{k_0}{E}, \quad y_k = \log \frac{k_0}{k} \tag{5}$$

and using (2) and (4), equation (1) becomes

$$\left.\begin{aligned} h(l,k)\,dk = h(l,y_k)\,dy_k = \Big[\log 2 \cdot e^{-\alpha l} \int_0^l e^{\alpha l'} 2 f(l', y_k)\,dl' + \\ + \delta(y_k)\, e^{-y_k} e^{-\alpha l}\Big]\, dy_k . \end{aligned}\right\} \tag{6}$$

Introducing this expression into the equation analogous to eq. (17) of B & H and transforming to the logarithmic variables (5) we obtain, proceeding in the same way as B & H, the final *integral equation* for the function $f(l,y)$

$$\left.\begin{aligned} f(l,y) = \alpha \log 2 \cdot e^{-\alpha l} \int_0^l dl' \int_0^{l-l'} dl''\, e^{\alpha(l'+l'')} \times \\ \times \int_0^y dy_k\, 2 f(l'', y_k)\, W(l'+1, y-y_k) + \\ + \alpha e^{-\alpha l} \int_0^l dl'\, e^{\alpha l'}\, W(l'+1, y) \end{aligned}\right\} \tag{7}$$

which is analogous to eq. (21) of B & H.

The solution of this equation, analogous to eqs. (22) and (23) of B & H, is given by

$$f(l,y) = \sum_{n=1}^{\infty} f_n(l,y) \tag{8}$$

with

$$\left.\begin{aligned} f_1(l,y) &= \alpha e^{-\alpha l}\int_0^l dl'\, e^{\alpha l'}\, W(l'+1,y) \\ f_n(l,y) &= \frac{(2\alpha\log 2)^n}{2\log 2}\, e^{-\alpha l}\int_0^l dl'\, e^{\alpha l'}\,\frac{l'^{n-1}(l-l')^{n-1}}{(n-1)!^2}\times \\ &\times\int_0^y \frac{(y-y')^{n-2}}{(n-2)!}\, W(l'+n,y')\,dy' \quad (n\geqq 2) \end{aligned}\right\} \tag{9}$$

which is proved in appendix I, where we also give the details of the numerical evaluation.

In Table 1 (cf. also fig. 17) we have tabulated the function $\bar{N}_f = 2f(l, y_c)$ giving the average number of positive *and* negative electrons which emerge from the thickness l with energies above the critical energy E_c and which we therefore denote by "fast" electrons.

2. Number of electrons below the critical energy.

The total average number of "slow" electrons, i. e. electrons with energies below the critical energy, arising from the secondary electrons with energies above E_c can be calculated in the same way as for electron-initiated showers. This number, which we shall denote by $\bar{N}_s$ (sec. el.), is given by (cf. eq. (15) in A)

$$\left.\begin{aligned} \bar{N}_s(\text{sec. el.}) &= 2\log 2\int_\gamma^l \frac{\partial f(L,y_c)}{\partial y}\,dL \\ \gamma &= \operatorname{Max}\left(l-\frac{1}{\log 2},0\right);\quad L = l-\frac{1-\dfrac{E}{E_c}}{\log 2} \end{aligned}\right\} \tag{10}$$

which is evaluated as described in § 1 in A using the values for $\frac{\partial f}{\partial y}$ given in Table 4. The results are given in Table 1.

Electrons with energies below the critical energy can also be produced by a second process. In the calculation of the number of "slow" electrons mentioned above it was assumed that above a certain critical energy E_c—equal to $1 \cdot 10^7$ e. V. in lead—the electrons can only lose energy by radiation and below E_c only by ionization. For the photons, however, this critical energy plays no role, the pair-production being the dominating process down to much lower energies—of the order 10^6 e. V. in lead. Below this energy the Compton and, later on, the photoelectric effect becomes the dominating process but, as discussed in § 1 in A, we consider it legitimate to neglect these two processes. A photon with energy above E_c has a certain probability of producing a pair of electrons one of which has an energy below E_c, and this electron has not been included either in $\bar{N}_f$ or in $\bar{N}_s$ (sec. el.). Furthermore, if the energy of the photon is below E_c, it can still produce a pair of electrons which will, however, both have energies below E_c. In part I we have neglected the "slow" electrons produced by this process, but on closer investigation it has appeared that they can contribute in some cases about 25 per cent of the total number of electrons.

As already discussed in A (see end of § 1) the total number of "slow" electrons will certainly exceed possible experimental values since these electrons will have a rather great chance of being scattered in the material. As a consequence of this fact one ought, therefore, to include only a certain fraction of these "slow" electrons in the later calculations. However, on the one hand it is extremely difficult to treat this scattering in a proper way, and on the other hand we shall see later on (cf. § 5) that the *form* of the Rossi curves does not depend critically on the number of slow electrons included.

In order to get some idea about the number of slow electrons of this second kind we can proceed in the following way. We first consider the primary photon and denote the total average number of slow electrons which it produces by $\bar{N}_s$ (prim. phot.). The probability that the primary photon with energy k_0 penetrates to a depth l' below the surface is $e^{-\alpha l'}$ and the probability that it in travelling the distance dl' will produce a pair where the positron has an energy between E_+ and $E_+ + dE_+$ is $\alpha dl' \frac{dE_+}{k_0}$. This last expression is, however, only valid for large values of k_0. For smaller values it is reduced by a factor $\theta(k_0)$, $0 \leqq \theta \leqq 1$, which depends on the energy k_0 (being 0 for $k_0 \leqq 2mc^2 = 2\mu$) and on the shower-producing material (cf. e. g. fig. 18 p. 201 in Heitler 1936). Using the formula (5) in A for the probability that an electron loses an energy between E'' and $E'' + dE''$ by ionization in travelling the distance $l'' = l - l'$ we have that the total average number of these slow *positrons* $\bar{N}_s^+$ (prim. phot.), i. e. positrons with energies below E_c, is given by

$$\left.\begin{aligned} \bar{N}_s^+(\text{prim. phot.}) &= \int_{\mu}^{m} dE \int_0^{l} dl' \times \\ \times \int_{\mu}^{k_0} dE_+ \, e^{-\alpha l'} \cdot \frac{\alpha}{k_0} \, \theta(k_0) \cdot \delta\left(E_+ - E - \beta(l-l')\right) \cdot \Delta(E_+ \leqq E_c) & \\ m &= \text{Min}(k_0, E_c) \\ \beta &= \log 2 \cdot E_c \\ \Delta(E_+ \leqq E_c) &= \begin{cases} 1 \text{ for } E_+ \leqq E_c \\ 0 \text{ for } E_+ > E_c \end{cases} \end{aligned}\right\} \quad (11)$$

where μ is the rest energy of the positron.

[1] In conformity with A, we shall denote by a symbol $\Delta(\ )$ a function which is 1 when the condition stated in the brackets is fulfilled, and 0 elsewhere.

This expression can be easily evaluated and we find, introducing

$$y_c = \log \frac{k_0}{E_c}, \tag{12}$$

$\bar{N}_s^+$ (prim. phot.) =

$$\left.\begin{aligned}
&= \theta(y_c)\left\{\left[1 - \log 2 \cdot e^{-y_c} \cdot l + \frac{\log 2}{\alpha} e^{-y_c}\right] - e^{-\alpha l}\left[1 + \frac{\log 2}{\alpha} e^{-y_c}\right]\right\} \\
&\qquad \text{for } y_c \leqq 0 \quad \text{and} \quad l \leqq \frac{e^{y_c}}{\log 2} \\
&= \theta(y_c)\left\{e^{-\alpha l}\left[\frac{\log 2\, e^{-y_c}}{\alpha}\left(e^{\frac{\alpha}{\log 2} e^{y_c}} - 1\right) - 1\right]\right\} \\
&\qquad \text{for } y_c \leqq 0 \quad \text{and} \quad l \geqq \frac{e^{y_c}}{\log 2} \\
&= \theta(y_c)\left\{e^{-y_c}\left(\left[1 - \log 2 \cdot l + \frac{\log 2}{\alpha}\right] - e^{-\alpha l}\left[1 + \frac{\log 2}{\alpha}\right]\right)\right\} \\
&\qquad \text{for } y_c \geqq 0 \quad \text{and} \quad l \leqq \frac{1}{\log 2} \\
&= \theta(y_c)\left\{e^{-\alpha l} e^{-y_c}\left[\frac{\log 2}{\alpha}\left(e^{\frac{\alpha^*}{\log 2}} - 1\right) - 1\right]\right\} \\
&\qquad \text{for } y_c \geqq 0 \quad \text{and} \quad l \geqq \frac{1}{\log 2}.
\end{aligned}\right\} \tag{13}$$

If the energy k_0 of the primary photon is greater than $2\,E_c$ and if one of the pair-electrons is produced with an energy below E_c the other electron must necessarily have an energy above E_c. In this case eq. (13) gives the total number of electrons (positive as well as negative).

In case $k_0 < E_c$ both pair-electrons will have energies below E_c and the total number of electrons is, therefore,

given by eq. (13) multiplied by a factor 2. In the range $E_c \leqq k_0 \leqq 2E_c$ it can either happen that both electrons have energies below E_c or that one has an energy below, the other above E_c, but not that both have energies above E_c. These facts we take into account roughly in the following way. For $y_c > 0$ (i. e. $k_0 > E_c$) we take $\theta(y_c) = 1$ and the total number equal to $\bar{N}_s^+$ (prim. phot.) as given in eq. (13), and for $y_c \leqq 0$ (i. e. $k_0 \leqq E_c$) we take the total number equal to $2\bar{N}_s^+$ (prim. phot.) as given in eq. (13), the numerical value of $\theta(y_c)$ being read off from fig. 18 p. 201 in Heitler (1936). Since for a given value of k_0, y_c depends on E_c, i. e. on the material used, the total number of slow electrons will thus depend on the material for $y_c \leqq 0$. In Table 3, which gives the sum of all the different sorts of electrons, the values for $y_c \leqq 0$ give the total average number $\bar{N}_s$ (prim. phot.) for lead, iron, and aluminium of the slow electrons calculated as just discussed. The corresponding values for $y_c > 0$, which are independent of E_c, depending only on y_c, are given in Table 1.

We next consider the secondary photons produced by the cascade multiplication from the primary photon. The average number of *secondary* photons which at the depth l' below the surface have energies between k and $k + dk$ is for $k \geqq E_c$ given by

$$\left.\begin{aligned} h_{\text{sec}}(l', k)\, dk &= h(l', k)\, dk - h(0, k)\, e^{-\alpha l'} \\ &= \log 2 \cdot \frac{dk}{k} e^{-\alpha l'} \int_0^{l'} e^{\alpha l''} \{ f_+(l'', k) + f_-(l'', k) \}\, dl'' \\ &\qquad (k \geqq E_c) \end{aligned}\right\} \quad (14)$$

(cf. eq. (1)), which is tabulated in Table 5 (cf. also fig. 18).

For $k \leqq E_c$ we have

$$h_{\text{sec}}(l', k)\, dk = \log 2 \cdot \frac{dk}{k} e^{-\alpha l'} \int_0^{l'} e^{\alpha l''} \{f_+(l'', E_c) + f_-(l'', E_c)\}\, dl'' \quad (k \leqq E_c) \tag{15}$$

where $f_+(l'', E_c) + f_-(l'', E_c)$ gives the average number of electrons which at the depth l'' below the surface have energies above E_c. In our approximation only such electrons can produce photons by bremsstrahlung. The probability for this process is given by the factor $\log 2 \cdot \frac{dk}{k}$. Finally $e^{-\alpha(l'-l'')}$ gives the probability for the photons produced at the depth l'' to penetrate the distance $l'-l''$. As already discussed above the pair production is the dominating process for the photons down to much lower energies than E_c. If, however, the Compton and the photoelectric effect are also taken into consideration it is found that the total absorption coefficient is roughly constant in the whole energy range considered and equal to the value of the absorption coefficient due to pair production for large energies, which is just α.

The total average number of slow *positrons* $\bar{N}_s^+$ (sec. phot.) arising from the secondary photons is then, in analogy to eq. (11) for the primary photon, given by the expression

$$\bar{N}_s^+(\text{sec. phot.}) = \int_\mu^{E_c} dE \int_0^l dl' \int_{2\mu}^{k_0} dk \int_\mu^{k_0} dE_+ \, h_{\text{sec}}(l', k) \cdot \frac{\alpha}{k} \theta(k) \times \times \delta\left(E_+ - E - \beta(l-l')\right) \cdot \Delta(E_+ \leqq E_c). \tag{16}$$

Here the integrations after dE and dE_+ can be evaluated and we find using (15) and introducing the logarithmic variables y_k and y_c given in eqs. (5) and (12)

$$\left.\begin{aligned}
\bar{N}_s^+(\text{sec. phot.}) &= \alpha \int_0^{l} dl' \,(1-\log 2\,(l-l')) \times \\
&\times \int_0^{y_c} dy_k\, h_{\text{sec}}(l', y_k)\,\theta(y_k)\cdot e^{y_k-y_c}\cdot \Delta\left(0 \leqq \beta\,(l-l') \leqq \frac{\beta}{\log 2}\right) + \\
&+ \alpha \int_0^{l} dl'\, h_{\text{sec}}(l', y_c) \int_{y_c}^{\log\left(\frac{k_0}{2\mu}\right)} dy_k\, \theta(y_c)\left[1 - e^{y_k-y_c}\left(\frac{\mu}{E_c} + \log 2(l-l')\right)\right] \times \\
&\times \Delta\left(0 \leqq \beta\,(l-l') \leqq \frac{\beta}{\log 2}\left(e^{y_c-y_k} - \frac{\mu}{E_c}\right)\right).
\end{aligned}\right\} \quad (17)$$

Here the first and second terms represent the contribution from those secondary photons which have energies above and below, respectively, the critical energy E_c. In order to obtain the total number of positive as well as negative electrons we therefore proceed in the same manner as in the case of the primary photon (cf. the discussion on p. 10). In the first term we take $\theta(y_k) = 1$ and do not multiply by 2 whereas we in the second term take the value for $\theta(y_k)$ obtained as described above and multiply by 2. By this procedure the first and second terms become independent and dependent, respectively, of the shower-producing material used and we shall therefore write

$$\bar{N}_s(\text{sec. phot.}) = \bar{N}_s(\text{sec. phot. ind.}) + \bar{N}_s(\text{sec. phot. dep.}) \quad (18)$$

The values for the first term obtained by numerical integration are given in Table 1. One might hope that the second term could be neglected, but a trial calculation showed this to be wrong and, as will be seen from Table 2 which gives the values for the second term, again obtained by numerical integration, this term can in some cases contribute about 20 per cent of the sum of all the different kinds of electrons, which is tabulated in Table 3.

3. The fluctuation formula.

All the numbers of electrons obtained so far are only *average* values and we must, therefore, now decide which fluctuation formula has to be used. By fluctuation formula we mean the formula giving the probability $P(N)$ that a shower contains just N positive as well as negative electrons.

Originally B & H took for this formula the well-known Poisson formula

$$P(N) = \frac{e^{-\bar{N}} \bar{N}^N}{N!} = P(N, l, y), \qquad (19)$$

$\bar{N}$ being the average number of secondary electrons, which formula follows directly assuming the secondary electrons to be independent of each other. The application of this formula to the fluctuation of the number of electrons in showers has later been criticized from various sides. In spite of the fact that the electrons are of course not independent of each other, it has, however, appeared as discussed in § 2 in A that the Poisson formula represents a good approximation for the small showers measured in counter experiments.

Since for photon-initiated showers there are only *secondary* electrons, the fluctuation formula is directly given by (19) with $\bar{N}$ equal to the sum of the average number of all the different kinds of electrons corresponding to a given value of l and $y_c = \log \frac{k_0}{E_c}$. This formula applies, however, only to *positive* values of y_c i.e. $k_0 > E_c$. For negative values of y_c, i.e. $k_0 \leqq E_c$, we can obtain the fluctuation formula as follows. In this energy region the primary photon can only undergo one single multiplication since already the two pair electrons produced in the first step will have

energies below E_c and can, therefore, in our approximation only lose energy due to ionization. The multiplication process, therefore, stops after the first step and the shower can at most contain *two* electrons. For the positive as well as the negative electron there are only two possibilities: either it is stopped by ionization or it comes out and the probability of the last event is therefore equal to the mean value $\bar{N}_s^+(\text{prim.phot.}) = \bar{N}_s^-(\text{prim.phot.})$. Treating the events of the positive and negative electrons coming out as independent we have consequently for negative values of y_c, i. e. $k_0 \leqq E_c$, the binomial distribution

$$\left.\begin{aligned} P(0,l,y_c) &= \left(1-\bar{N}_s^+\right)^2 \\ P(1,l,y_c) &= 2\bar{N}_s^+\left(1-\bar{N}_s^+\right) \\ P(2,l,y_c) &= \bar{N}_s^{+2} \\ P(N,l,y_c) &= 0 \text{ for } N \geqq 3 \end{aligned}\right\} \quad y_c \leqq 0 \qquad (20)$$

with $\bar{N}_s^+ = \bar{N}_s^+$ (prim. phot.).

It could be objected that it is not correct to use the Poisson formula (19) for *small* thicknesses l since in this case practically only one transformation, i. e. formation of a single pair, will take place so that we cannot observe more than *two* electrons. It would, therefore, be more correct to use (20) with $\bar{N}_s^+ \to \frac{\bar{N}}{2}$. For small values of l we have, however, $\bar{N} \ll 1$ and thus, neglecting third and higher powers of $\bar{N}$, the Poisson formula reduces to

$$P(0) \sim 1-\bar{N}+\frac{\bar{N}^2}{2}, \quad P(1) \sim \bar{N}-\bar{N}^2, \quad P(2) \sim \frac{\bar{N}^2}{2}$$

and

$$P(N) = 0 \text{ for } N \geqq 3$$

which agrees to the first power with (20) which gives for $\bar{N}_s^+ \to \frac{\bar{N}}{2}$:

$$P(0) = 1 - \bar{N} + \frac{\bar{N}^2}{4}, \quad P(1) = \bar{N} - \frac{\bar{N}^2}{2}, \quad P(2) = \frac{\bar{N}^2}{4}$$

and

$$P(N) = 0 \quad \text{for} \quad N \geqq 3.$$

As soon as l becomes so large that $\bar{N}^2$ cannot be neglected it is, however, also necessary to take the next transformations into account, which will allow *more* than two electrons to emerge. We shall therefore use the Poisson formula for all positive values of y_c.

4. Energy spectrum of the incident photons.

The expressions (19) and (20) give the probability for a photon with the definite energy k_0 to produce a shower with just N electrons. What is measured in all coincidence experiments is, however, the *mean* effect produced by all the incident photons (plus, of course, all the incident electrons) hitting the material during the time of investigation. Let us denote the probability of the primary photons having an energy between k_0 and $k_0 + dk_0$ by $F(k_0)\, dk_0$. The average probabilities with respect to this spectrum is then given by

$$\left.\begin{aligned} \bar{P}(N, l) &= \int_0^\infty P(N, l, k_0)\, F(k_0)\, dk_0 \\ \int_0^\infty F(k_0)\, dk_0 &= 1 \qquad \text{i. e.} \qquad \sum_{N=0}^{\infty} \bar{P}(N) = 1 \end{aligned}\right\} \quad (21)$$

where $P(N, l, k_0)$ is given by (19) and (20).

The form of the photon spectrum is, however, poorly known. As already mentioned in the introduction it is experimentally very difficult to isolate the effects of the photons from those of the electrons. The cascade theory allows, however, to make a rough estimate of the form.

We first assume that all electrons and photons found at sea-level are produced by multiplication in the atmosphere of the primary radiation reaching the earth from outside. From the geomagnetic effects one concludes, as is well-known, that most, if not all, of this radiation consists of energetic electrons[1]. From the cascade theory Heitler[2] and Nordheim[3] have estimated the spectrum of these primary electrons and found that it can be approximated by a power law

$$f(E_0)\,dE_0 = \text{const.} \times \frac{dE_0}{E_0^{1+\gamma}} \tag{22}$$

where γ depends only very slowly on E_0 and is of the order $1-2$. If $h(l, k, E_0)\,dk$ denotes the average number of photons which at a depth l below the top of the atmosphere have energies between k and $k+dk$, the photons being produced from a primary electron with energy E_0, the photon energy spectrum at the depth l is simply given by

$$\left.\begin{aligned} F(l, k)\,dk &= dk \int_M^\infty h(l, k, E_0)\, f(E_0)\, dE_0 \\ M &= \text{Max}\,(k, E_\varphi) \end{aligned}\right\} \tag{23}$$

where

$$E_\varphi = 1.9 \times 10^{10} \cos^4 \varphi \quad \text{e. V.} \tag{24}$$

is the minimum energy required by an electron to penetrate the magnetic field of the earth and reach the top of the atmosphere in the vertical direction at the geomagnetic latitude φ. For $k \geq E_c^{\text{air}} = 1.5 \times 10^8$ e. V., which is the critical energy for air, $h(l, k, E_0)$ is given by a formula analogous to (14)[4], and for $k \leqq E_c^{\text{air}}$ by a formula analogous

1) Johnson (1938).
2) Heitler (1937).
3) Nordheim (1938).
4) Cf. eq. (16) in B & H and our Tables 7 and 8.

to (15). Introducing (22) in (23) and transforming to logarithmic variables analogous to (5) we have therefore

$$\left.\begin{aligned} F(l,k)\,dk &= \text{const.}\,\frac{dk}{k^{1+\gamma}}\int_{M_k}^{\infty} n(l,y_k)\,e^{-\gamma y_k}\,dy_k \\ y_k &= \log\frac{E_0}{k};\quad M_k = \operatorname{Max}\left(0,\ y_k^{\varphi} = \log\frac{E_\varphi}{k}\right) \end{aligned}\right\} k \geqq E_c^{\text{air}}$$

$$\left.\begin{aligned} F(l,k)\,dk &= \frac{\text{const}}{(E_c^{\text{air}})^{\gamma}}\,\frac{dk}{k}\int_{M_c}^{\infty} h(l,y_c)\,e^{-\gamma y_c}\,dy_c \\ y_c &= \log\frac{E_0}{E_c^{\text{air}}};\quad M_c = \operatorname{Max}\left(0,\ y_c^{\varphi} = \log\frac{E_\varphi}{E_c^{\text{air}}}\right) \end{aligned}\right\} k \leqq E_c^{\text{air}} \qquad (25)$$

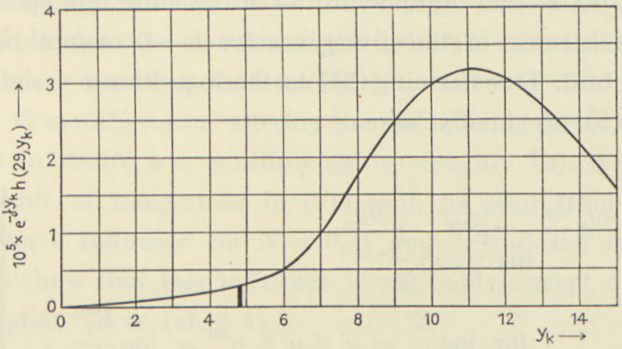

FIG. 1. *The integrand from eq. (25) corresponding to sea-level, $l = 29$.*

In fig. 1 is shown the common integrand for $l = 29$ corresponding to sea-level and, since, from (24), $E_\varphi \leqq 1.9\times10^{10}$ e.V., we have

$$0 \leqq y_k^{\varphi} \leqq y_c^{\varphi} \leqq \log\frac{1.9\times10^{10}}{1.5\times10^{8}} \sim 4{,}8. \qquad (26)$$

It is seen from the figure that the integrals are very nearly constant, independent of both k and the latitude φ, and the cascade theory thus yields for the photon spectrum at sea-level

$$\left.\begin{aligned} F(k)\,dk &= \frac{1}{\log\frac{E_c^{\text{air}}}{E'}+\frac{1}{\gamma}}\,\frac{dk}{k} \quad \text{for} \quad E' \leqq k \leqq E_c^{\text{air}} \\ F(k)\,dk &= \frac{E_c^{\text{air}}}{\log\frac{E_c^{\text{air}}}{E'}+\frac{1}{\gamma}}\,\frac{dk}{k^{1+\gamma}} \quad \text{for} \quad E_c^{\text{air}} \leqq k \\ &\int_{E'}^{\infty} F(k)\,dk = 1 \end{aligned}\right\} \quad (27)$$

where E′ is the—unknown—lower limit for this spectrum which because of the divergence for $k \to 0$ cannot be put equal to 0. Transforming (27) to the logarithmic variable y_c from (5), we finally have

$$\left.\begin{aligned} F(y_c)\,dy_c &= \frac{1}{\log\frac{E_c^{\text{air}}}{E'}+\frac{1}{\gamma}}\,dy_c \\ &\text{for} \quad \log\frac{E'}{E_c} = y_c' \leqq y_c \leqq y_c^{\text{air}} = \log\frac{E_c^{\text{air}}}{E_c} \\ F(y_c)\,dy_c &= \frac{e^{\gamma y_c^{\text{air}}}}{\log\frac{E_c^{\text{air}}}{E'}+\frac{1}{\gamma}}\,e^{-\gamma y_c}\,dy_c \\ &\text{for} \quad \log\frac{E_c^{\text{air}}}{E_c} = y_c^{\text{air}} \leqq y_c \end{aligned}\right\} \quad (28)$$

where E_c is the critical energy for the *material*.

For the numerical values we have taken $\gamma = 1.5$ as in A, and $E_c^{\text{air}} = 1.5 \times 10^8$ e. V. With this value and the expression (1) in A for E_c, we have[1]

$$y_c^{\text{air}} = \log \frac{E_c^{\text{air}}}{E_c} = \log \frac{1.5\,Z}{8} = \left\{ \begin{array}{l} 2.7 \text{ for } Pb \\ 1.6 \text{ for } Fe \\ 0.9 \text{ for } Al \end{array} \right\} \quad (29)$$

For the lower limit of the spectrum we shall take the value $E' = 10^7$ e. V. With this value we have

$$y_c' = \log \frac{E'}{E_c} = \log \frac{Z}{80} = \left\{ \begin{array}{l} 0.0 \text{ for } Pb \\ -1.1 \text{ for } Fe \\ -1.8 \text{ for } Al \end{array} \right\} \quad (30)$$

The assumptions under which the spectrum is deduced are certainly valid down to this energy. Presumably they also hold down to energies of the order 10^6 e. V. From (28) it is seen, however, that taking $E' = 10^6$ e. V. instead of 10^7 e. V. mainly means altering the normalizing factor (from 0.296 to 0.176, i. e. multiplying by roughly $^2/_3$). Altering the limit of integration in (21) will, as seen from (20), only have influence for $N = 0$, 1 and 2, and the calculations show that this influence is negligible, except on the absorption curve (cf. § 5).

The spectrum given in (28) was, however, deduced under the assumption that the whole of the soft component observed at sea-level arises from cascade multiplication of the primary electrons in the atmosphere. From this assumption and from the cascade theory it follows, as shown by

[1] We note that these values deviate slightly from the corresponding ones for the electron spectrum given in eq. (27) in A. This is because we have here used a theoretically deduced spectrum, while the electron spectrum was deduced partly from theoretical arguments and partly from experiments.

Heitler[1] and also from the preceeding calculations, that at sea-level the latitude effect[2] of the soft component should be zero, which Heitler also finds in agreement with experiments. On the other hand Euler and Heisenberg state in their report[3] that at sea-level the soft component shows a latitude effect of the same order as the hard component, i. e. 10 per cent. It is perhaps worth noting that these contradictory conclusions are based on one and the same experiment, viz. that of Auger and Leprince-Ringuet[4]. Looking at the experimental curves of these authors we find it, however, because of the large fluctuations, very difficult to draw any positive conclusions regarding the existence of a latitude effect of the soft component at sea-level. Furthermore, Johnson[5] concludes on the basis of more recent experiments that the whole of the latitude effect observed must be attributed to the hard component. It thus seems that experiments do not contradict the assumption that the whole of the soft component found at sea-level is produced by cascade multiplication of the primary electrons.

On the other hand, however, we must expect that a smaller or greater fraction has its origin in the secondary effects of the hard component, i. e. the mesons. These particles can theoretically produce cascade showers of electrons and photons by three processes. First, the meson is assumed to be unstable and to disintegrate into an electron and a neutrino, the electron at once starting an

1) Heitler (1937).

2) The latitude effect is measured by $\frac{I_{50} - I_0}{I_{50}}$, where I_φ is the intensity at the geomagnetic latitude φ.

3) Euler and Heisenberg (1938).

4) Auger and Leprince-Ringuet (1934).

5) Johnson (1938).

ordinary shower. Second, a meson can in an elastic collision eject secondary electrons which will also at once start ordinary showers. Third, a meson may be absorbed by a heavy particle, the whole energy being emitted in the form of a photon. The experimental verification of the first process is now beyond any doubt[1]. The second process is also well established[2),3)], whereas it seems that the third process does not occur in nature or at any rate only with an extremely small probability[3)]. In air the first process is certainly the dominating process and from the spectrum of the mesons as a function of e. g. the atmospheric pressure it would be easy to calculate from the cascade theory the contribution of the hard component to the photon spectrum at sea-level. The meson spectrum in high altitudes is, however, poorly known at present experimentally, and since it is not yet known by what processes the mesons are produced[4)] the spectrum cannot be estimated theoretically either. We believe, however, that the meson contribution to the photon spectrum would not alter its form appreciably from that calculated above as the contribution of the primary electrons. Finally, it will later appear that the result does not seem to depend critically on the form of the spectrum. We shall, therefore, base the following calculations on the spectrum given in (27).

5. General discussion of results and comparison with experiments.

The expressions given in (21) cannot yet be directly compared with experiments, since they only give the aver-

1) Williams and Roberts (1940) and Rossi (1939).

2) Wilson (1938), and others.

3) Lovell (1939).

4) Generally it is assumed that they are produced by the soft com-

age probabilities for a shower emerging after a thickness l to consist of *just* N electrons. What is measured is, however, the weighted probabilities for showers to consist of *at least* N electrons. We thus have to calculate

$$\bar{P}(\geq N, l) = \sum_{N'=N}^{\infty} g_{N'} \bar{P}(N', l) \tag{31}$$

where the weight g_N is the probability for a shower consisting of N electrons to produce a coincidence. As discussed in § 4 in A these weights, the so-called *geometrical factors*, are rather difficult to estimate, and we shall, therefore, again take the non-vanishing g_N's equal to unity throughout.

In figs. 2, 4 and 6 we give the curves $\bar{P}(\geq N, l)$[1] for lead, iron, and aluminium and for $N = 1$, 2, 3, and 4 calculated for the spectrum (27) with $\gamma = 1.5$, $E_c^{\text{air}} = 1.5 \times \times 10^8$ e. V., and the lower limit $E' = 10^7$ e. V. (With the same spectrum but with $E' = 10^6$ e. V., the curves will, as discussed on p. 19, differ only by a constant factor). Comparing the curves with the corresponding curves for electron-initiated showers (see figs. 4 and 5 in A, and fig. 19 in appendix III in this paper) it is seen, that the general shape and the positions of the maxima and their variation with N is the same for electron- and photon-initiated showers. The absolute magnitudes are, however, different. For lead the electron curves lie roughly 50 per cent. higher than the photon curves. This is partly due to the contribution from the primary electrons and partly due to the electron spectrum being in favour of somewhat higher energies than

ponent in high altitudes, but it has also been proposed that they are produced by primary protons (Alfven (1939), Johnson (1939)).

[1] Normalized so that $\sum_{N=0}^{\infty} \bar{P}(N, l) \equiv 100\ \%$.

the photon spectrum. For aluminium, on the other hand, the photon curves lie above the electron curves, because

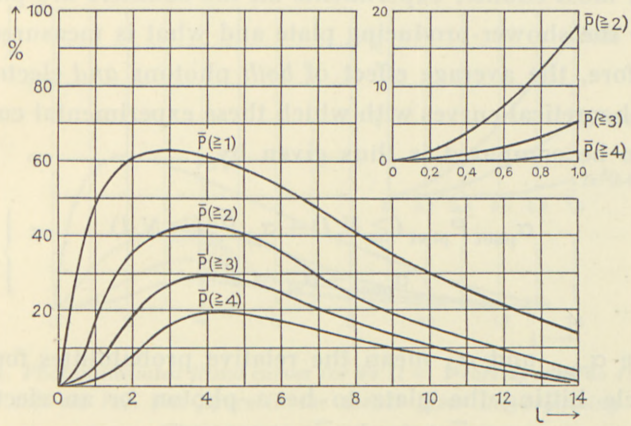

FIG. 2. *Photon-initiated* ROSSI *curves for Pb (l = 1 corresponds to 4.06 g/cm² Pb or 0.358 cm Pb). The figure in the corner gives the beginning of the* ROSSI *curves on a larger scale.*

of the fact that we have included more slow electrons in the photon curves than in the electron curves. These new

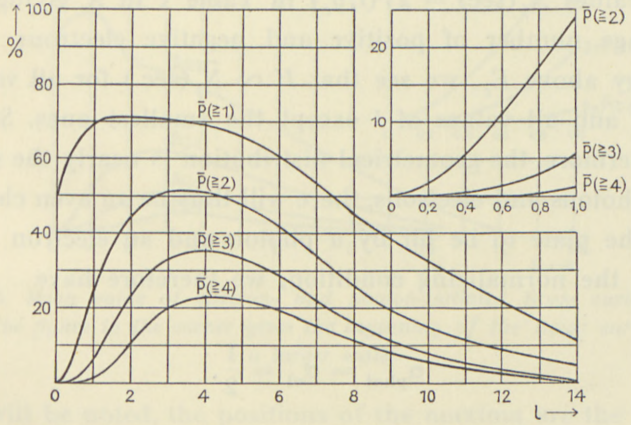

FIG. 3. *Mean value of electron- and photon-initiated* ROSSI *curves for Pb. The figure in the corner gives the beginning of the* ROSSI *curves on a larger scale.*

slow electrons contribute far more in aluminium than in lead and will thus outweigh the other two effects.

In most counter experiments all the counters are placed *below* the shower-producing plate and what is measured is, therefore, the average effect of *both* photons *and* electrons. The theoretical curves with which these experimental curves are to be compared is thus given by

$$\left.\begin{aligned} &\alpha_{\text{phot}}\,\overline{P}_{\text{phot}}\,(\geqq N, l) + \alpha_{\text{el}}\,\overline{P}_{\text{el}}\,(\geqq N, l) \\ &\alpha_{\text{phot}} + \alpha_{\text{el}} = 1 \end{aligned}\right\} \quad (32)$$

where α_{phot} and α_{el} mean the relative probabilities for the particle hitting the plate to be a photon or an electron, respectively, and $\overline{P}_{\text{phot}}$ and $\overline{P}_{\text{el}}$ are the expression given in (31) for photon- and electron-initiated showers, respectively.

If we compare for *electron*-initiated showers the values $H_{\text{el}}(l, y_c)$ in Table 8 giving the average number of photons with energy above E_c corresponding to $y_c = \log \frac{E_0}{E_c}$ with the values $\overline{N}_f(\text{sec}) = 2f(l, y_c)$ in Table 1 in A giving the average number of positive and negative electrons with energy above E_c, we see that $H \backsim \overline{N}_f(\text{sec.})$ for all values of y_c and all values of l except the smallest ones. Since, furthermore, the geometrical distribution is nearly the same for photons and electrons, there will thus be an even chance for the plate to be hit by a photon and an electron and, from the normalizing condition, we therefore have

$$\alpha_{\text{phot}} = \alpha_{\text{el}} = \frac{1}{2}. \quad (33)$$

As will be noted, this statement is independent of whether we assume that the whole soft component at sea-level is

produced by cascade multiplication of the primary electrons or whether some part is produced by the hard component.

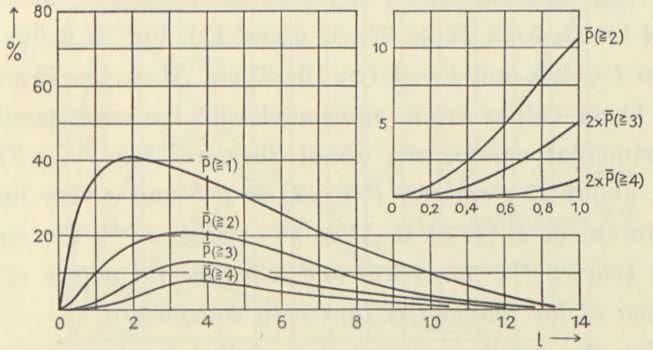

FIG. 4. *Photon-initiated ROSSI curves for Fe ($t = 1$ corresponds to 10 g/cm² Fe or 1.26 cm Fe). The figure in the corner gives the beginning of the ROSSI curves on a larger scale.*

In figs. 3, 5, and 7, we give the curves $\frac{1}{2}\,\bar{P}_{\text{phot}} + \frac{1}{2}\,\bar{P}_{\text{el}}$ for lead, iron, and aluminium and for $N = 1, 2, 3$, and 4.

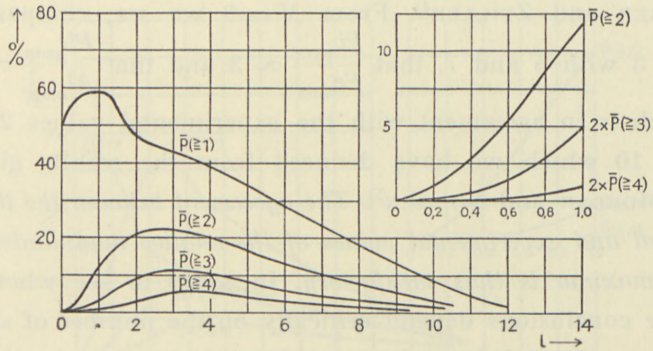

FIG. 5. *Mean value of electron- and photon-initiated ROSSI curves for Fe. The figure in the corner gives the beginning of the ROSSI curves on a larger scale.*

As will be noted, the positions of the maxima are the same as for the corresponding curves for electron-initiated showers (see figs. 4, and 5 in A and fig. 19 in appendix III). For

Pb the position varies very little from $N = 2$ to $N = 4$ and lies at values of l between 3.5 and 4.5 ($\sim 1.2 - 1.4$ cm *Pb* $\sim$ 14—18 g/cm^2 *Pb*). For *Fe* it lies between $l = 2.5$ and $l = 4$ ($\sim$ 3—5 cm *Fe* $\sim$ 25—40 g/cm^2 *Fe*). For *Al* it lies between $l = 2.5$ and $l = 4$ ($\sim$ 16—27 cm *Al* $\sim$ 45—75 g/cm^2 *Al*). These values are in agreement with the corresponding experimental values, viz. about 20 g/cm^2 for $\bar{P}$ ($\geqq 2$) in *Pb*[1], about 35 g/cm^2 for $\bar{P}$ ($\geqq 2$) in *Fe*[2] and a very broad maximum of $\bar{P}$ ($\geqq 3$) in *Al* at 50—100 g/cm^2 [3]. *The agreement between the theoretical and experimental values of the position of the maxima is thus very satisfactory.*

For the relative magnitudes of the maxima we now find better agreement than in A. From fig. 3 we see that in *Pb* $\frac{\bar{P}(\geqq 3)_{\max}}{\bar{P}(\geqq 2)_{\max}} \sim 0.7$ in agreement with the experimental value 0.5 which we have deduced subtracting the hard component by extrapolation from the results given by Geiger and Zeiller[4]. From $N = 3$ we see, comparing figs. 3 with 5 and 7, that $\frac{Pb_{\max}}{Fe_{\max}} \sim 3$ and that $\frac{Pb_{\max}}{Al_{\max}} \sim 8$ which is in agreement with the experimental values 2—3 and 10 which we have deduced from the results given by Morgan and Nielsen[5]. *The agreement between the theoretical and experimental values of the relative magnitudes of the maxima is thus satisfactory.* In order to see whether these conclusions depend critically on the number of slow electrons included we have performed some trial calculations with various values of this number. The results

1) Schwegler (1935), see also our Fig. 9.
2) Priebsch (1935).
3) Morgan and Nielsen (1936).
4) Geiger and Zeiller (1937).
5) Morgan and Nielsen (1936).

showed that the position of the maxima was not altered at all and that the relative magnitudes of the maxima

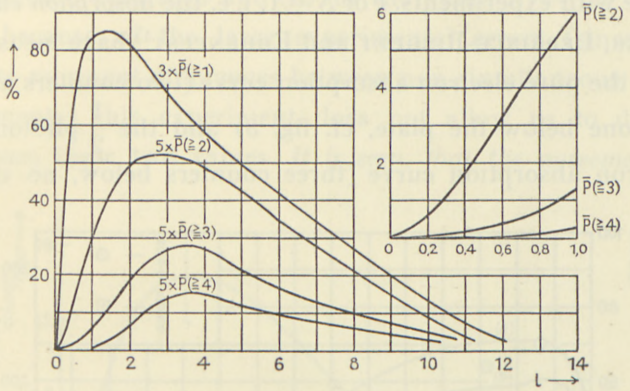

FIG. 6. *Photon-initiated* ROSSI *curves for Al (t = 1 corresponds to 18 g/cm² Al or 6.71 cm Al). The figure in the corner gives the beginning of the* ROSSI *curves on a larger scale.*

for constant N and different materials only varied slightly. The relative magnitude of the maxima for the same material

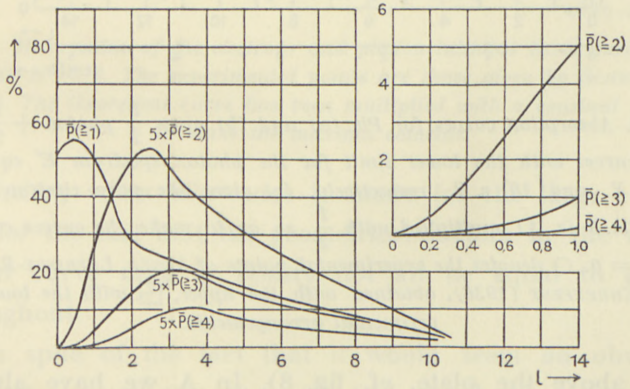

FIG. 7. *Mean value of electron- and photon-initiated* ROSSI *curves for Al. The figure in the corner gives the beginning of the* ROSSI *curves on a larger scale.*

and different values of N varied somewhat, however, as would be expected, since increasing the values of the total N means favouring large showers.

Until now we have discussed only the general features of the theoretical curves. We shall now compare the whole shape with experiments. For $N = 1$, i. e. the *absorption curves*, Auger, Leprince-Ringuet and Ehrenfest[1] have measured both the pure electron absorption curve (two counters above and one below the plate, cf. fig. 8) and the $\frac{1}{2}$ photon $+\frac{1}{2}$ electron absorption curve (three counters below, no coun-

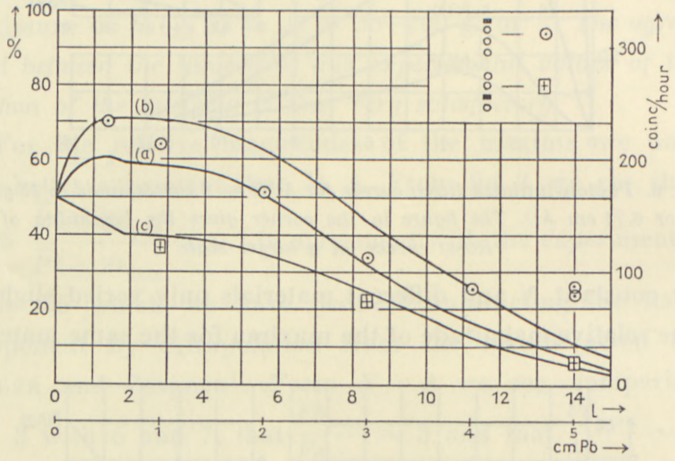

Fig. 8. *Absorption curves for Pb. (a) and (b) gives* $\frac{1}{2}$ *photon* $+\frac{1}{2}$ *electron curves with the lower limit for the photon spectrum* E' *equal to* 10^6 *e. V. and* 10^7 *e. V., respectively. (c) gives the pure electron curve (cf. Fig. 3 in A) multiplied with* $\frac{1}{2}$*, so as to make the curves coincide for* $l = 0$. ⊙ *denotes the experimental points of Auger, Leprince-Ringuet and Ehrenfest (1936), obtained with the upper,* ⊞ *with the lower experimental arrangements.*

ters above the plate, cf. fig. 8). In A we have already compared the theoretical and experimental pure electron absorption curve. In fig. 8 we give the theoretical $\frac{1}{2}$ photon $+\frac{1}{2}$ electron absorption curve and the experimental points

[1] Auger, Leprince-Ringuet and Ehrenfest (1936).

(normalized so that they agree for $l = 0$). Curve (a) corresponds to the value $E' = 10^6$ e. V. for the lower limit of the photon spectrum and (b) to the value $E' = 10^7$ e. V., but because of the large experimental errors (since the points represent differences between non-simultaneous measurements) this experiment does not allow us to decide between these two values. *It is seen, that the agreement is*

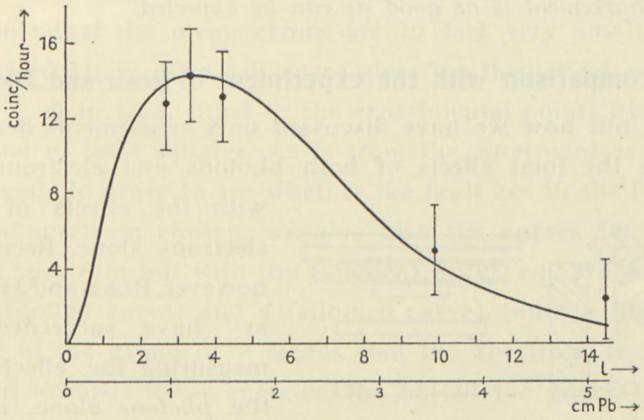

FIG. 9. *Mean value of the electron- and photon-initiated* ROSSI *curves for Pb with* $N = 2$. *The experimental points are those given by* SCHWEGLER *(1935). The theoretical curve has been multiplied with a constant so as to make the maxima coincide.*

satisfactory when allowance is made for the large errors and for the fact that the geometrical factors in the theoretical curve need in reality not all be equal to unity throughout.

In spite of the fact that it would seem an obvious problem to separate the soft and the hard component also for the other ROSSI curves, this question has only been investigated, as far as we know, in the experiment of SCHWEGLER[1] already discussed in A (cf. page 536 and

[1] SCHWEGLER (1935).

fig. 2). In fig. 9 we give Schwegler's experimental points for the $\overline{P}$ (≥ 2, l) curve in lead and the corresponding theoretical $\frac{1}{2}$ photon $+\frac{1}{2}$ electron curve, since with his arrangement both the photons and the electrons contribute to the coincidences. Also here the large statistical errors are caused by the fact that the points are differences between non-simultaneous measurements. *As is seen, the agreement is as good as can be expected.*

6. Comparison with the experiment of Rossi and Jánossy.

Until now we have discussed only experiments dealing with the total effects of both photons and electrons, or with the effects of the electrons alone. Recently, however, Rossi and Jánossy[1] have succeeded in measuring the effects of the *photons* alone, using the method of anticoincidences. In fig. 10 their experimental arrangement is shown. The five upper counters A are in parallel, as are also the two lower counters D. An anticoincidence is now a coincidence between B, C, and D, which is *not* accompanied by a simultaneous discharge of the counter battery A. It is to be noted, that the amplifier is so built that the anticoincidenses are measured *directly*, which procedure makes the statistical errors very small in contrast to the usual difference method (cf. e. g. the measure-

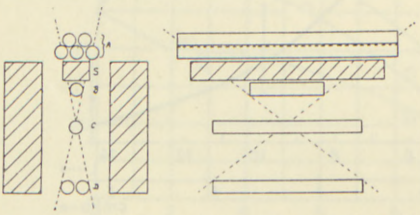

Fig. 10. *Experimental arrangement of Rossi and Jánossy.*

[1] Private communication. We wish to thank Professor Rossi and Dr. Jánossy for kindly sending us their manuscript before publication. (A short survey of the experiments has later been given at the Symposium on cosmic rays held at the University of Chicago, June 1939; see Blackett and Rossi, 1939).

ments of SCHWEGLER discussed above). What is measured by this arrangement is obviously showers containing at least one electron and initiated by *photons* or, at any rate by *non-ionizing* rays, since both primary electrons and primary mesons would discharge the counter battery A and could thus not produce an anticoincidence.

In fig. 11 is shown the number of anticoincidences per hour as a function of the thickness of the lead plate s; we note that the mean errors are in fact very small, as discussed above. The full curve gives the theoretical curve $\overline{P}\ (\geqq 1, l)$ in lead, fitted to the experimental points by the method of least squares. As is seen, the agreement is not too good. In order to see whether the fault lies in the form of the spectrum chosen, we give also the curves for the same spectrum but with the exponent γ (cf. eq. 27) equal to 2 (dotted curve) and 4 (stippled curve). Since a higher value of the exponent γ means that the spectrum is displaced towards lower energies, the tail of the curves will lie lower the higher the value of γ, as is also seen from the figure. It is, however, not possible in this way to obtain curves which have as high and as narrow a maximum as the experimental points indicate. Looking at the geometrical arrangement of the counters (fig. 10) we see, however, that most, though not necessarily all, of the electrons have to penetrate up to five counterwalls (each of which consists of 0.1 mm. copper foil plus a certain amount of pyrex glass) besides a certain amount of wood and iron from the framework of the apparatus. It is, therefore, likely that only energetic electrons are measured, the less energetic ones being stopped in the counterwalls. ROSSI and JÁNOSSY themselves estimate that only electrons with energies above 10^7 e. V., which is just the critical energy in lead, are registered,

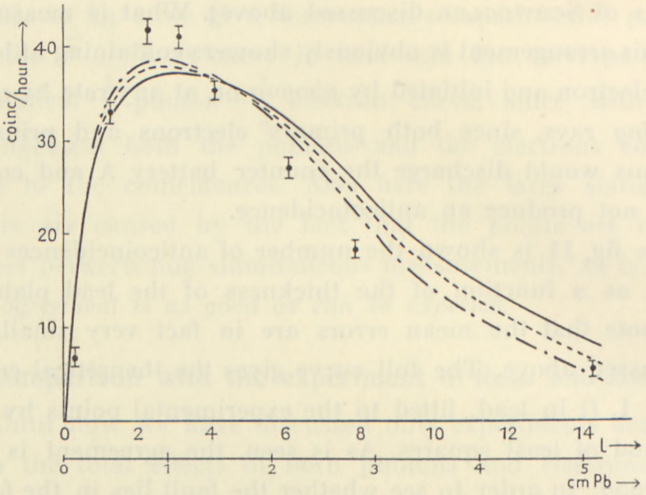

Fig. 11. *Theoretical photon-initiated Rossi curves ($N = 1$) in Pb fitted by the method of least squares to the experimental points of Rossi and Jánossy. Both "fast" and "slow" electrons included. Full, dotted and stippled curves correspond to $\gamma = 1.5$, 2 and 4, respectively.*

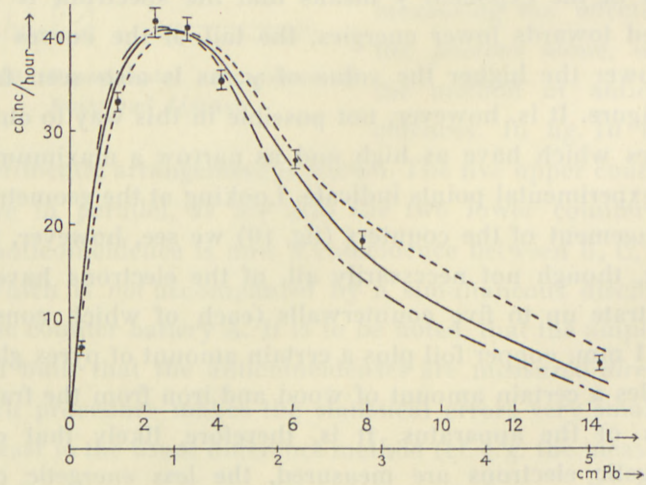

Fig. 12. *Theoretical photon-initiated Rossi curves ($N = 1$) in Pb fitted by the method of least squares to the experimental points of Rossi and Jánossy. Only "fast" electrons included. Full, dotted and stippled curve corresponds to $\gamma = 1.5$, 1 and 2, respectively.*

and we therefore have to compare the experimental points with the theoretical curve $\overline{P}$ (≥ 1, l) calculated with $\overline{N} = \overline{N}_f$, where $\overline{N}_f$ (given in Table 1) is the average number of "fast" electrons. The result is shown in fig. 12 where the full curve corresponds to the spectrum (27) with $\gamma = 1.5$, the dotted curve to $\gamma = 1$, and the stippled curve to $\gamma = 2$, all curves fitted by the method of least squares. As is seen, the curve with $\gamma = 1.5$ fits the experimental points much better than the curves with $\gamma = 1$ or 2, *the agreement being almost better than could be expected.*

If we use, however, the so-called χ^2-test of goodness of fit[1] the agreement turns out to be less good than the figure indicates. If p_i is some measured number and π_i the theoretically expected number, χ^2 is given by

$$\chi^2 = \sum_i \frac{(p_i - \pi_i)^2}{\pi_i}.$$

Here p_i is the directly measured total number of counts and π_i is the number given in the figures *plus* the zero-point number, both multiplied by the number of hours counted. From the values given by Rossi and Jánossy we find, that $\chi^2 = 50.5$ for the 1.5 curve in fig. 12. From a table of the distribution of χ^2 [2] we see, however, that the probability for a χ^2 value as high as or higher than this value is much smaller than 0.001 (the number of degrees of freedom being here one less than the number of points, 8). This large value of χ^2 is, however, mainly due to the first experimental point the deviation of which is not clearly brought out in the figure because of the steep rise of the curve at the beginning. If we regard this single point as

[1] Cf. e. g. Fisher (1938), chap. IV.

[2] See e. g. Fisher and Yates (1938), table IV.

false and omit it, χ^2 reduces to 19.8, the corresponding probability being of the order of 0.01, which is still somewhat too small. We think, however, that, because of the many uncertainties and approximations, the goodnees of fit obtained is all that can reasonably be expected here.

Comparing the figs. 11 and 12 we see that the effect of including all the "slow" electrons is to make the curves flatter and broader, the tail being higher in proportion to the maximum. If we included only a certain fraction of the "slow" electrons, assuming the rest to be scattered away (cf. p. 7), we should thus obtain nearly the correct form with a value of γ somewhat higher than 1.5. We cannot conclude, therefore, that γ must necessarily have the value 1.5.

In this connection we note that the value 10^7 e. V. which the electrons necessarily must have, according to Rossi and Jánossy, in order to penetrate the counter walls etc. seems to us to be rather high. Furthermore, it is quite possible that we have to use a higher exponent in the spectrum. Because of the backward effect it is possible that not all the photons which hit the plate give rise to anticoincidences. This backward effect would be the more pronounced the more energetic the photons. We should thus expect that the anticoincidences are mainly produced by the less energetic photons, i. e. by a spectrum with a somewhat higher value of γ.

Finally, we observe that the theoretical curve fits the experimental points even for thicknesses as great as 5 cm. lead. *This means, that if the hard component contains neutral mesons at all, the probability for these particles to produce ionizing rays must be extremely small.* For, if the neutral mesons did produce such rays they would obviously give rise to anticoincidences and since the neutral particles would

be very penetrating they would contribute mainly to the tail of the curve and thus quite alter its form.

To test this point directly, Rossi and Jánossy measured the number of coincidences when a 5 cm. lead plate was placed (1) between the counters A and B and (2) between B and C, a 10 cm. lead plate being located between C and D throughout. A positive difference will then indicate that non-ionizing rays have produced penetrating ionizing rays. In fact, they found a positive, but very small difference. However, as they point out themselves, further control experiments are necessary in order to allow the conclusion that we have really to do with neutral mesons transforming themselves into charged mesons. On the other hand, this process has already been searched for by Lovell[1], but with negative result.

7. Special discussion of the beginning of the Rossi curves.

As already discussed in A (§ 6) several investigators have found that, if the number of coincidences is plotted for different elements as a function of the thickness on a scale proportional to the product of Z^2 and the number of atoms per cm.^{3} (i. e. practically on an l-scale), the points all lie on the same curve for small thicknesses, up to $l \sim 1$[2]. In fig. 13 we plot $\frac{1}{2}\overline{P}_{\text{phot}}(\geqq 2, l) + \frac{1}{2}\overline{P}_{\text{el}}(\geqq 2, l)$, and in fig. 14 $\frac{1}{2}\overline{P}_{\text{phot}}(\geqq 3, l) + \frac{1}{2}\overline{P}_{\text{el}}(\geqq 3, l)$ for lead, iron, and aluminium for $0 \leqq l \leqq 1$. As is seen, *the three curves do not coincide at all.* Only for thicknesses of the order $l < \frac{1}{4}$, are the differences very small. *Taking the zero point*

[1] Lovell (1939).

[2] Hu Chien Shan (1937); Hu Chien Shan, Kisilbasch and Ketiladge (1937); Watase (1937).

effects and the statistical errors into account one would, therefore, expect identical curves in agreement with what is found in the experiments quoted. In the experiments of *Hu* the curves seem, however, to be identical also for larger values of l, up to about $l = 1$, for which value the theoretical curves deviate considerably. In A we suggested that this

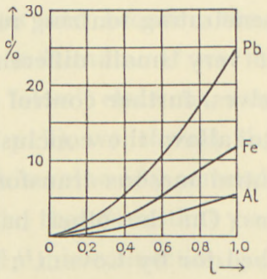

Fig. 13. *Mean value of electron- and photon-initiated Rossi curves ($N = 2$) for small thicknesses of Pb, Fe and Al.*

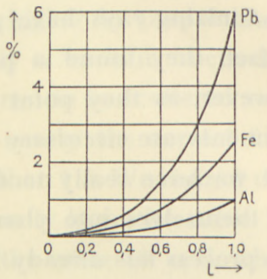

Fig. 14. *Mean value of electron- and photon-initiated Rossi curves ($N = 3$) for small thicknesses of Pb, Fe and Al.*

discrepancy might possibly be explained in the following way. In the experiments mentioned above coincidences of at least three particles were measured. The proportionality with Z^2 was then explained by a simultaneous arrival of a photon and an electron, the photon transforming into a pair which, together with the electron, gives rise to a coincidence. This argument was, however, false because both the influence of the energy spectrum of the primary radiation and of the fluctuations was neglected. We can now evaluate the probability, which we shall denote by $\overline{P}_{\text{el} \times \text{phot}} (\geqq N, l)$, for a simultaneously arriving pair of one electron and one photon producing a common shower containing at least N electrons. This probability is given by

$$\left.\begin{aligned}\overline{P}_{\text{el}\times\text{phot}}(\geqq N,l) &= \sum_{i=0}^{N} \overline{P}_{\text{el}}(i,l)\cdot\overline{P}_{\text{phot}}(\geqq N-i,l)+\overline{P}_{\text{el}}(\geqq N+1,l)\\ &= \sum_{i=0}^{N} \overline{P}_{\text{phot}}(i,l)\cdot\overline{P}_{\text{el}}(\geqq N-i,l)+\overline{P}_{\text{phot}}(\geqq N+1,l)\end{aligned}\right\} \quad (35)$$

because $\geqq N$ electrons means *either* just 0 electrons in the shower produced by the electron and $\geqq N$ in the shower produced by the photon, *or* just 1 in the first and $\geqq N-1$ in the second shower and so on, *or* finally just N in the first and $\geqq 0$ in the second shower, the probability of which is just given by the sum. To this has, however, to be added the probability for $\geqq N+1$ electrons in the first and $\geqq 0$ in the second shower, which is just given by the last term.

Because of the symmetry in electrons and photons we must, however, also consider the case that two electrons or two photons arrive simultaneously. The corresponding probabilities, which we shall denote by $\overline{P}_{\text{el}\times\text{el}}(\geqq N,l)$ and $\overline{P}_{\text{phot}\times\text{phot}}(\geqq N,l)$, are given by formulae analogous to (35). Finally, we have to take the mean of $\overline{P}_{\text{el}\times\text{el}}$, $\overline{P}_{\text{phot}\times\text{phot}}$, and $\overline{P}_{\text{el}\times\text{phot}}$ with the weights $\frac{1}{4}, \frac{1}{4}, \frac{1}{2}$, because the probabilities of the events el × el, phot × phot, and el × phot have the ratios 1 : 1 : 2. The results for $N=2$ and $N=3$ is shown in figs. 15 and 16 for lead, iron, and aluminium and, as is seen, *the three curves do not coincide at all.* Since, in fact, we have to take the weighted mean of $\frac{1}{2}\overline{P}_{\text{el}}+\frac{1}{2}\overline{P}_{\text{phot}}$ and the last curve with some presumably small weight for the last one, this means *that we cannot explain the result found by Hv.* As already pointed out in A (end of § 6) we have, however, to remember that *the effect of the hard component has not*

been subtracted in these experiments and that we do not know at present what contribution the hard component gives to the beginning of the Rossi curves. Only further experiments[1] can clear up this point and before they have been made it is not possible to draw any conclusions regarding the beginning of the Rossi curves.

A further difficulty in comparing the theoretical with the experimental Rossi curves for small thicknesses is presented by the zero point effect. As discussed in A (§ 4) this effect is due partly to the final resolving power, partly to the air showers, and partly to showers from the walls, the ceiling, the floor, etc. As a rule, the zero point effect is eliminated by subtracting a constant amount from the counts measured. As regards that part of the zero point effect which is caused by the air-showers, wall-showers, etc. coming from above, it is clear that this procedure is not quite correct since the plate will give rise to a multiplication of these showers which would be different in different materials. This fact is seen from fig. 15 where the finite starting point comes from the fact that two simultaneously arriving electrons also can produce double coincidences without any material present. We see e. g. that in lead this zero point effect increases by a factor 2.6 when the thickness of the plate is increased from $l = 0$ to $l = 1$. For three simultaneously arriving particles we would have curves analogous to figs. 15 and 16, and we thus see that, in the experiments of *Hv*, we had to subtract different zero point effects for different materials and for different thicknesses. Unfortunately, we should thus obtain

1) We suggest that the method of anticoincidences (see p. 30) would also be a valuable method in isolating the effects of the hard component from those of the soft one.

curves with the wrong dependence on material, the aluminium curves lying above the lead curves, since the zero point effect is multiplied more in lead than in aluminium.

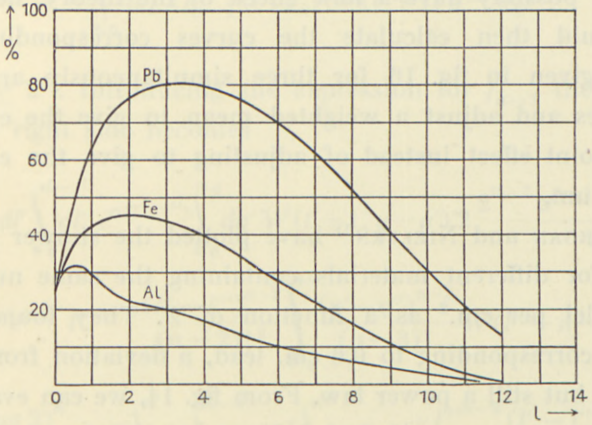

FIG. 15. *Simultaneously arriving photons and electrons. ROSSI curves corresponding to* $\frac{1}{4}\bar{P}_{el\times el}(\geqq 2,l)+\frac{1}{4}\bar{P}_{phot\times phot}(\geqq 2,l)+\frac{1}{2}\bar{P}_{phot\times el}(\geqq 2,l)$ *for Pb, Fe and Al.*

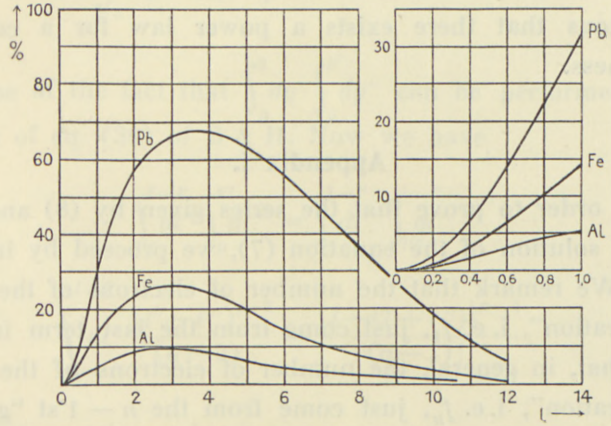

FIG. 16. *Simultaneously arriving photons and electrons. ROSSI curves corresponding to* $\frac{1}{4}\bar{P}_{el\times el}(\geqq 3,l)+\frac{1}{4}\bar{P}_{phot\times phot}(\geqq 3,l)+\frac{1}{2}\bar{P}_{phot\times el}(\geqq 3,l)$ *for Pb, Fe and Al. The figure in the corner gives the beginning of the ROSSI curves on a larger scale.*

We think, therefore, that the explanation must be sought in the fact that the hard component also contributes for these small layers. If this contribution were known we should possibly have a new check of the theory, because we could then calculate the curves corresponding to those given in fig. 16 for three simultaneously arriving particles and adjust a weighted mean to give the correct zero point effect instead of adjusting to give the correct maximum.

Morgan and Nielsen[1] have plotted the shower intensities for different materials containing the same number of nuclei per cm.^{2} as a function of Z. They found, for layers corresponding to 0.6 cm. lead, a deviation from the Z^2 law but still a power law. From fig. 14, we can evaluate the same curve and we find, in fact, a power law but with a power 5 instead of Morgan and Nielsen's value ~ 3.2. If, however, we plot the corresponding curve for other thicknesses, we do not find a power law. It seems thus fortuitous that there exists a power law for a certain thickness.

Appendix I.

In order to prove that the series given by (8) and (9) is the solution of the equation (7), we proceed by induction. We remark that the number of electrons of the first "generation", i. e. f_1, just come from the last term in (7) and that, in general, the number of electrons of the n'th "generation", i. e. f_n, just come from the $n-1$'st "generation", i. e. f_{n-1}. We therefore have only to prove that

[1] Morgan and Nielsen (1937).

$$f_n(l, y) = \alpha \log 2\, e^{-\alpha l} \int_0^l dl' \int_0^{l-l'} dl''\, e^{\alpha(l'+l'')} \times$$

$$\times \int_0^y dy_k\, 2 f_{n-1}(l'', y_k)\, W(l'+1, y-y_k)$$

for $n \geqq 2$[1]. Introducing the expression for f_{n-1} the term on the right side becomes

$$\alpha \log 2\, e^{-\alpha l} \int_0^l dl' \int_0^{l-l'} dl''\, e^{\alpha(l'+l'')} \int_0^y dy'\, W(l'+1, y-y')\, 2\, \frac{2^{n-1}\alpha^{n-1}(\log 2)^{n-2}}{2} \times$$

$$\times e^{-\alpha l''} \int_0^{l''} dl'''\, e^{\alpha l'''} l'''^{n-2} \frac{(l''-l''')^{n-2}}{(n-2)!^2} \int_0^{y'} \frac{(y'-y'')^{n-3}}{(n-3)!}\, W(l'''+n-1, y'')\, dy'' =$$

$$= \frac{(2\alpha \log 2)^n}{2 \log 2}\, e^{-\alpha l} \int_0^l dl' \int_0^{l-l'} dl''\, e^{\alpha l'} \int_0^{l''} dl'''\, e^{\alpha l'''} \frac{l'''^{n-2}(l''-l''')^{n-2}}{(n-2)!^2} \times$$

$$\times \int_0^y \frac{(y-y')^{n-2}}{(n-2)!}\, W(l'+l'''+n, y')\, dy'$$

because of the fact that $\int_0^y dy' \int_0^{y'} dy''$ can be performed by means of eq. (39) of B & H. Now we have

$$\int_0^{l-l'} dl'' \int_0^{l''} dl''' = \int_0^{l-l'} dl''' \int_{l'''}^{l-l'} dl''$$

and

$$\int_{l'''}^{l-l'} dl'' \frac{(l''-l''')^{n-2}}{(n-2)!} = \frac{(l-(l'+l'''))^{n-1}}{(n-1)!},$$

so our expression reduces to

[1] Strictly speaking, the case $n = 2$ has to be considered separately but, since $\lim_{n \to 1} f_n(l, y) = f_1(l, y)$, which is easily seen, we can confine ourselves to the general case.

$$\frac{(2\alpha\log 2)^n}{2\log 2}\, e^{-\alpha l}\int_0^{l} dl' \int_0^{l-l'} dl''\, \frac{(l-(l'+l''))^{n-1}}{(n-1)!}\, e^{\alpha(l'+l'')}\, \frac{l''^{n-2}}{(n-2)!}\times$$

$$\times \int_0^{y} \frac{(y-y')^{n-2}}{(n-2)!}\, W(l'+l''+n, y')\, dy'.$$

Introducing $l'+l'' = l''$ as a new variable and using the fact that

$$\int_0^{l} dl' \int_0^{l-l'} dl'' = \int_0^{l} dl'' \int_0^{l''} dl'$$

and

$$\int_0^{l''} dl' \frac{(l''-l')^{n-2}}{(n-2)!} = \frac{l''^{n-1}}{(n-1)!}$$

we obtain at once

$$\frac{(2\alpha\log 2)^n}{2\log 2}\, e^{-\alpha l}\int_0^{l} dl''\, e^{\alpha l''}\, \frac{(l-l')^{n-1}}{(n-1)!}\, \frac{l''^{n-1}}{(n-1)!}\times$$

$$\times \int_0^{y} \frac{(y-y')^{n-2}}{(n-2)!}\, W(l''+n, y')\, dy'$$

which, writing l' instead of l'', is just $f_n(l, y)$.

For the numerical evaluation of the functions $f_n(l, y)$ it is convenient to write them in another form for $n \geq 2$. Introducing the definition of W, interchanging the order of integration, one integration can be performed and we are left with

$$f_n(l, y) = \frac{(2\alpha\log 2)^n}{2\log 2}\, \frac{1}{(n-1)!^3} \int_0^{l} dl' \left\{e^{\alpha(l-l')}\, l'^{n-1}(l-l')^{n-1}\right\}\times$$

$$\times \left[\int_0^{y} dy'\, \frac{e^{-y'}\, y'^{l'+n-1}(y-y')^{n-1}}{(l'+n-1)!}\right]^{*}.$$

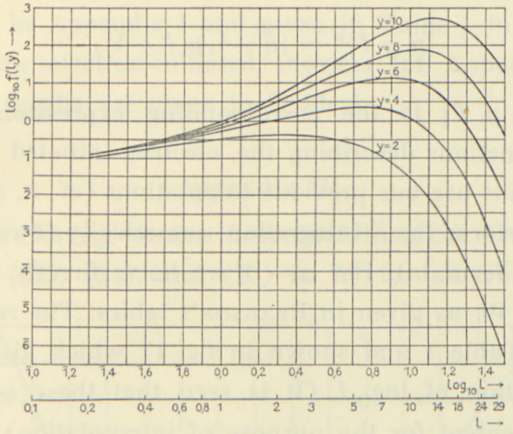

FIG. 17. *Photon-initiated showers. $f(l, y)$ as a function of l in a double logarithmic scale for different values of $y = \log \frac{k_0}{E}$.*

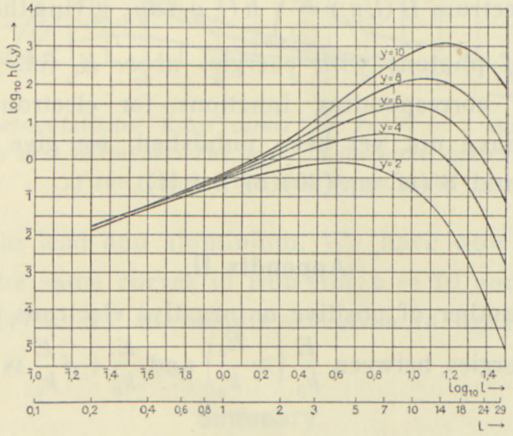

FIG. 18. *Photon-initiated showers. $h(l, y)$ as a function of l in a double logarithmic scale, for different values of $y = \log \frac{k_0}{k}$.*

Comparing this expression with eq. (28) in A we see that

$$[n, y, l']^* = [n-1, y, l'+1],$$

where $[n, y, l']$ is the corresponding expression in the $f_n(l, y)$ functions describing the electron-initiated showers. We can thus use our previous calculations (cf. A, Appendix I) and perform the l' integration numerically (by means of SIMPSON's formula). For $n = 1$ we have directly used the values of W, as given in PEARSON's tables. The results are given in Table 1 and shown in fig. 17 which gives $\log_{10} f$ as a function of $\log_{10} l$. (It is seen that these scales are very convenient for the purpose of interpolation).

Inserting the values of $f(l, y_k)$ in (6) we obtain by numerical integration the values given in Table 5 and fig. 18 for the differential photon spectrum $h(l, y_k)$. For the sake of comparison, we have also calculated the total photon spectrum $H(l, y_c) = \int_0^{y_c} h(l, y_k)\, dy_k$ giving the average number of photons with energies *above* E_c (cf. Table 6). Since the corresponding functions for electron-initiated showers have not yet been published, we give them in Tables 7 and 8 (cf. eq. (20) of B & H).

Appendix II.

The number of positive *or* negative electrons which at l have energies between $\frac{E}{k_0}\left(>\frac{E_c}{k_0}\right)$ and $\frac{E}{k_0} + d\frac{E}{k_0}$ is given by

$$k_0\, p(l, E)\, d\frac{E}{k_0} = -\frac{\partial f(l, y)}{\partial E}\, dE = e^y \frac{\partial f(l, y)}{\partial y} \cdot d\frac{E}{k_0}$$

$$y = \log \frac{k_0}{E}.$$

We have calculated $k_0\, p\,(l, E)$ from the values of $f(l, y)$ obtained in Appendix I and given in Table 1 in the same way as for electron-initiated showers (cf. Appendix II in A). The results are given in Table 4.

Appendix III.

In A we have given the theoretical Rossi curves $\bar{P}\,(\geqq N, l)$ (cf. eqs. (22), (24), and (27) in A) for electron-initiated

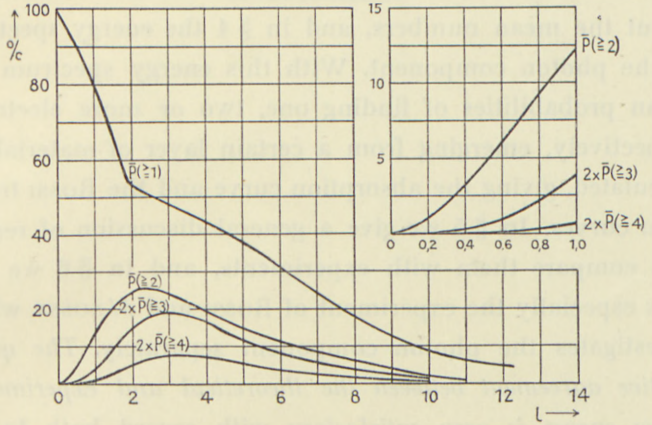

Fig. 19. *Electron-initiated Rossi curves for Fe. ($l = 1$ corresponds to 10 g/cm² Fe or 1.26 cm. Fe). The figure in the corner gives the beginning of the Rossi curves on a larger scale.*

showers in lead and aluminium. We have now also calculated the same curves in iron (for $\alpha = 10$ and $\gamma = 1.5$, cf. eq. (24) in A); the results are given in fig. 19.

Summary.

We have calculated the theoretical Rossi curves for showers initiated by the photon component of the cosmic rays. The calculations follow those of Arley[1] dealing with

[1] Arley (1938), quoted as A.

the theoretical Rossi curves of electron-initiated showers. In § 1 we work out from the cascade theory of showers, in the form put forward by Bhabha and Heitler, the average numbers of "fast" electrons and photons, i. e. particles having energies above the critical energy of the shower producing material. In § 2 we calculate in the same way as in A the corresponding numbers of "slow" particles, i. e. particles having energies less than the critical energy. In § 3 we discuss the fluctuations of the number of electrons about the mean numbers, and in § 4 the energy spectrum of the photon component. With this energy spectrum the mean probabilities of finding one, two or more electrons, respectively, emerging from a certain layer of material are calculated, giving the absorption curve and the Rossi transition curves. In § 5 we give a general discussion of results and compare them with experiments, and in § 6 we discuss especially the experiment of Rossi and Jánossy which investigates the photon component separately. *The quantitative agreement between the theoretical and experimental Rossi curves is very satisfactory* with regard both to the shape of the curves and to their dependence on the material. In § 6 we also discuss the possible existence of neutral mesons. We conclude that they either cannot exist in the cosmic radiation or must have an extremely small probability for transforming to charged particles (mesons or secondary electrons). Finally we discuss, in § 7, the beginning of the Rossi curves and find that the Z^2 law found by Hu and others for small thicknesses cannot be understood from the cascade theory. In this connection we point out, however, that before the contribution from the hard component to the beginning of the Rossi curves in different materials has been investigated experimentally, it is im-

possible to draw any further conclusions. New experiments regarding this point are, therefore, extremely desirable. Furthermore, we point out that difficulty is presented by the subtraction of the zero point effect.

In conclusion, we wish to thank Professor NIELS BOHR for his kind interest in this work.

References.

Alfvén 1939, Nature **143**, 435.
Arley 1938, Proc. Roy. Soc. A **168**, 519 (quoted as A).
Arley and Heitler 1938, Nature **142**, 158.
Auger and Leprince-Ringuet 1934, Int. Conf. Nucl. Physics, London.
Auger, Leprince-Ringuet and Ehrenfest 1936, J. Phys. Radium **7**, 58.
Bhabha and Heitler 1937, Proc. Roy. Soc. A **159**, 432 (quoted as B & H).
Blackett and Rossi 1939, Rev. Mod. Phys. **11**, 277.
Carlson and Oppenheimer 1937, Phys. Rev. **51**, 220.
Euler and Heisenberg 1938, Erg. exakt. Naturwiss. **17**, 1.
Fisher 1938, Statistical Methods for Research Workers, London.
Fisher and Yates 1938, Statistical Tables, London.
Geiger and Zeiller 1937, Z. Phys. **105**, 517.
Heitler 1936, Quantum Theory of Radiation, Oxford.
Heitler 1937, Proc. Roy. Soc. A **161**, 261.
Hu Chien Shan 1937, Proc. Roy. Soc. A **158**, 581.
Hu Chien Shan, Kisilbasch and Ketiladge 1937, Proc. Roy. Soc. A **161**, 95.
Johnson 1938, Rev. Mod. Phys. **10**, 193.
Johnson 1939, J. Franklin Inst. **227**, 37.
Kemmer 1938, Proc. Camb. Phil. Soc. **34**, 354.
Lovell 1939, Proc. Roy. Soc. A **172**, 568.
Morgan and Nielsen 1936, Phys. Rev. **50**, 882.
Morgan and Nielsen 1937, Phys. Rev. **52**, 568.
Møller 1938, Nature **142**, 290.
Nordheim 1938, Phys. Rev. **53**, 694.
Priebsch 1935, Z. Phys. **95**, 102.
Rossi 1939, Rev. Mod. Phys. **11**, 296.
Schwegler 1935, Z. Phys. **96**, 62.
Watase 1937, Proc. Phys. Math. Soc. Japan **19**, 749.
Williams and Roberts 1940, Nature **145**, 102.
Wilson 1938, Nature **142**, 73.

TABLE 1. *Photon-initiated showers. The average number* $\bar{N}$ *of "fast" (f) and "slow" (s) electrons (positive* **and** *negative) as functions of* t *and* $y_c = \log \frac{k_0}{E_c}$. $\bar{N}_f = 2f(t, y_c)$, $\bar{N}_s$ *(sec. el.) the number of "slow" electrons arising from the secondary electrons,* $\bar{N}_s$ *(prim. phot.) from the primary photon and* $\bar{N}_s$ *(sec. phot. ind.) that part, arising from the secondary photons, which is independent of the material.*

t	y_c		2	4	6	8	10
0.2		$\bar{N}_f$	0.200	0.234	0.242	0.246	0.248
		$\bar{N}_s$ (sec. el.)	0.003	0.00030	0.00013	0.00007	0.000046
		$\bar{N}_s$ (prim. phot.)	0.0142	0.00193	0.00026	0	0
		$\bar{N}_s$ (sec. phot. ind.)	0.00043	0.00066	0.00069	0.00069	0.00069
0.4		$\bar{N}_f$	0.350	0.432	0.462	0.482	0.502
		$\bar{N}_s$ (sec. el.)	0.011	0.0019	0.0010	0.00074	0.00056
		$\bar{N}_s$ (prim. phot.)	0.0247	0.00335	0.00045	0	0
		$\bar{N}_s$ (sec. phot. ind.)	0.0025	0.0041	0.0045	0.0046	0.0046
0.6		$\bar{N}_f$	0.484	0.636	0.716	0.782	0.848
		$\bar{N}_s$ (sec. el.)	0.025	0.0063	0.0041	0.0034	0.0028
		$\bar{N}_s$ (prim. phot.)	0.0319	0.00432	0.00058	0	0
		$\bar{N}_s$ (sec. phot. ind.)	0.0070*	0.013 *	0.015 *	0.016 *	0.016 *
0.8		$\bar{N}_f$	0.598	0.858	1.01	1.16	1.32
		$\bar{N}_s$ (sec. el.)	0.045	0.0163	0.012	0.010	0.010
		$\bar{N}_s$ (prim. phot.)	0.0361	0.00489	0.0007	0	0
		$\bar{N}_s$ (sec. phot. ind.)	0.015 *	0.027 *	0.032 *	0.034 *	0.036 *
1.0		$\bar{N}_f$	0.694	1.07	1.36	1.65	1.96
		$\bar{N}_s$ (sec. el.)	0.072	0.034	0.026	0.024	0.027
		$\bar{N}_s$ (prim. phot.)	0.0378	0.0051	0.0007	0	0
		$\bar{N}_s$ (sec. phot. ind.)	0.028	0.0482	0.059	0.063	0.069
2.0		$\bar{N}_f$	0.926	2.26	4.08	6.44	9.38
		$\bar{N}_s$ (sec. el.)	0.349	0.340	0.399	0.463	0.576
		$\bar{N}_s$ (prim. phot.)	0.0241	0.0033	0	0	0
		$\bar{N}_s$ (sec. phot. ind.)	0.115 *	0.237 *	0.371 *	0.489 *	0.67 *
3.0		$\bar{N}_f$	0.940 *	3.40 *	8.44 *	16.6 *	30.0 *
		$\bar{N}_s$ (sec. el.)	0.730	1.07	1.50	2.28	3.43
		$\bar{N}_s$ (prim. phot.)	0.0132	0	0	0	0
		$\bar{N}_s$ (sec. phot. ind.)	0.180	0.478	0.94	1.80	2.92

* Interpolated.

Table 1 *(continued).*

l \ y_c		2	4	6	8	10
5.0	$\bar{N}_f$	0.494	4.70 *	19.6	56.4 *	144
	$\bar{N}_s$ (sec. el.)	0.889	3.17	8.28	18.6	38.2
	$\bar{N}_s$ (prim. phot.)	0.0040	0	0	0	0
	$\bar{N}_s$ (sec. phot. ind.)	0.155	0.97	3.35	7.8	16.7
10.0	$\bar{N}_f$	0.0556	2.10 *	22.8	147 *	838
	$\bar{N}_s$ (sec. el.)	0.169	3.16	23.9	112	514
	$\bar{N}_s$ (prim. phot.)	0.0002	0	0	0	0
	$\bar{N}_s$ (sec. phot. ind.)	0.0271	0.835	5.75	30.5	147
14.0	$\bar{N}_f$	0.00830	0.618 *	10.2	115 *	1070
	$\bar{N}_s$ (sec. el.)	0.0426	1.34	14.9	126	1070
	$\bar{N}_s$ (prim. phot.)	0	0	0	0	0
	$\bar{N}_s$ (sec. phot. ind.)	0.0033 *	0.281 *	3.8 *	27.5 *	280 *
18.0	$\bar{N}_f$	0.00105	0.121 *	3.10	49.2 *	748
	$\bar{N}_s$ (sec. el.)	0.00448	0.31	5.4	72.4	1080
	$\bar{N}_s$ (prim. phot.)	0	0	0	0	0
	$\bar{N}_s$ (sec. phot. ind.)	0.00052	0.071	1.40	13.7	229
24.0	$\bar{N}_f$	$4.66 \cdot 10^{-5}$	0.00760*	0.358	9.24 *	234
	$\bar{N}_s$ (sec. el.)	$2.5 \cdot 10^{-4}$	0.026	0.86	19.1	490
	$\bar{N}_s$ (prim. phot.)	0	0	0	0	0
	$\bar{N}_s$ (sec. phot. ind.)	$2.3 \cdot 10^{-5}$*	0.0055 *	0.21 *	3.0 *	83 *
29.0	$\bar{N}_f$	$3.5 \cdot 10^{-6}$*	0.00056*	0.047 *	2.0 *	69 *
	$\bar{N}_s$ (sec. el.)	$5 \cdot 10^{-6}$	0.0022	0.15	6.0	190
	$\bar{N}_s$ (prim. phot.)	0	0	0	0	0
	$\bar{N}_s$ (sec. phot. ind.)	$1.5 \cdot 10^{-6}$	0.0008	0.034	0.73	26

* Interpolated.

TABLE 2. *Photon-initiated showers.* $\bar{N}_s$ *(sec. phot. dep.), that part of the number of "slow" electrons (positive* ***and*** *negative), arising from the secondary photons, which is dependent of the material, as Functions of* l *and* $y_c = \log \frac{k_0}{E_c}$ *for* ***Pb****,* ***Fe*** *and* ***Al****.*

l \ y_c			2	4	6	8	10
0.2	$\bar{N}_s$ (sec. phot. dep.)	*Al*	0.0020	0.0024	0.0024	0.0024	0.0024
		Fe	0.0013	0.0016	0.0016	0.0016	0.0016
		Pb	0.00045	0.00054	0.00054	0.00054	0.00054

TABLE 2 *(continued).*

l \ y_c		2	4	6	8	10
0.4	$\bar{N}_s$ (sec. phot. dep.) *Al*	0.012	0.015	0.015	0.015	0.015
	Fe	0.0077	0.0099	0.010	0.010	0.010
	Pb	0.0028	0.0032	0.0034	0.0036	0.0036
0.6	$\bar{N}_s$ (sec. phot. dep.) *Al*	0.032	0.041	0.045	0.046	0.047
	Fe	0.021	0.028	0.030	0.031	0.031
	Pb	0.0079	0.0093	0.010	0.011	0.011
0.8	$\bar{N}_s$ (sec. phot. dep.) *Al*	0.063	0.079	0.089	0.093	0.094
	Fe	0.042	0.053	0.059	0.062	0.063
	Pb	0.016	0.019	0.021	0.023	0.024
1.0	$\bar{N}_s$ (sec. phot. dep.) *Al*	0.11	0.14	0.16	0.17	0.18
	Fe	0.073	0.093	0.11	0.11	0.12
	Pb	0.026	0.034	0.038	0.042	0.045
2.0	$\bar{N}_s$ (sec. phot. dep.) *Al*	0.40	0.65	0.94	1.2	1.6
	Fe	0.27	0.43	0.63	0.82	1.1
	Pb	0.096	0.16	0.22	0.30	0.39
3.0	$\bar{N}_s$ (sec. phot. dep.) *Al*	0.66	1.4	2.7	4.3	6.7
	Fe	0.44	0.93	1.8	2.9	4.5
	Pb	0.15	0.35	0.63	1.1	1.7
5.0	$\bar{N}_s$ (sec. phot. dep.) *Al*	0.66	3.0	8.9	21	43
	Fe	0.44	2.0	5.9	14	29
	Pb	0.17	0.81	2.4	5.5	11
10.0	$\bar{N}_s$ (sec. phot. dep.) *Al*	0.16	3.1	23	98	380
	Fe	0.11	2.1	15	65	250
	Pb	0.040	0.83	5.6	25	110
14.0	$\bar{N}_s$ (sec. phot. dep.) *Al*	0.031	1.3	16	110	560
	Fe	0.021	0.84	11	70	380
	Pb	0.0076	0.32	3.9	26	150
18.0	$\bar{N}_s$ (sec. phot. dep.) *Al*	$5.0 \cdot 10^{-3}$	0.33	5.8	51	360
	Fe	$3.3 \cdot 10^{-3}$	0.22	3.9	34	240
	Pb	$1.2 \cdot 10^{-3}$	0.088	1.6	14	96
24.0	$\bar{N}_s$ (sec. phot. dep.) *Al*	$2.8 \cdot 10^{-4}$	0.032	0.91	13	140
	Fe	$1.9 \cdot 10^{-4}$	0.021	0.61	8.4	94
	Pb	$6.6 \cdot 10^{-5}$	0.0085	0.24	3.2	36
29.0	$\bar{N}_s$ (sec. phot. dep.) *Al*	$2.2 \cdot 10^{-5}$	$3.8 \cdot 10^{-3}$	0.16	2.9	40
	Fe	$1.5 \cdot 10^{-5}$	$2.6 \cdot 10^{-3}$	0.10	1.9	27
	Pb	$5.9 \cdot 10^{-6}$	$9.9 \cdot 10^{-4}$	0.042	0.76	12

TABLE 3. *Photon-initiated showers. The total average numbers* $\bar{N}$ *for* $y_c = \log \frac{k_0}{E_c}$ *for* **Pb**, **Fe** *and* **Al**. *For* $y_c \leq 0$

l \ y_c			−3	−2	−1
0.2	$\bar{N}$	*Al*	$2.49 \cdot 10^{-3}$	$2.47 \cdot 10^{-2}$	0.0869
		Fe	$4 \cdot 10^{-4}$	$1.07 \cdot 10^{-2}$	0.0549
		Pb	0	$1.0 \cdot 10^{-3}$	0.0183
0.4	$\bar{N}$	*Al*	$2.21 \cdot 10^{-3}$	$2.19 \cdot 10^{-2}$	0.124
		Fe	$3.3 \cdot 10^{-4}$	$9.51 \cdot 10^{-3}$	0.0780
		Pb	0	$9 \cdot 10^{-4}$	0.0260
0.6	$\bar{N}$	*Al*	$1.97 \cdot 10^{-3}$	$1.95 \cdot 10^{-2}$	0.117
		Fe	$2.9 \cdot 10^{-4}$	$8.44 \cdot 10^{-3}$	0.0744
		Pb	0	$8 \cdot 10^{-4}$	0.0247
0.8	$\bar{N}$	*Al*	$1.74 \cdot 10^{-3}$	$1.73 \cdot 10^{-2}$	0.104
		Fe	$2.6 \cdot 10^{-4}$	$7.49 \cdot 10^{-3}$	0.0657
		Pb	0	$7 \cdot 10^{-4}$	0.0219
1.0	$\bar{N}$	*Al*	$1.54 \cdot 10^{-3}$	$1.53 \cdot 10^{-2}$	0.0926
		Fe	$2.3 \cdot 10^{-4}$	$6.44 \cdot 10^{-3}$	0.0585
		Pb	0	$6 \cdot 10^{-4}$	0.0195
2.0	$\bar{N}$	*Al*	$8.5 \cdot 10^{-4}$	$8.40 \cdot 10^{-3}$	0.0508
		Fe	$1.3 \cdot 10^{-4}$	$3.65 \cdot 10^{-3}$	0.0321
		Pb	0	$3.5 \cdot 10^{-4}$	0.0107
3.0	$\bar{N}$	*Al*	$4.6 \cdot 10^{-4}$	$4.69 \cdot 10^{-3}$	0.0278
		Fe	0	$2.04 \cdot 10^{-3}$	0.0176
		Pb	0	$1.9 \cdot 10^{-4}$	0.00586
5.0	$\bar{N}$	*Al*	$1.4 \cdot 10^{-4}$	$1.39 \cdot 10^{-3}$	$8.41 \cdot 10^{-3}$
		Fe	0	$6 \cdot 10^{-4}$	$5.31 \cdot 10^{-3}$
		Pb	0	0	$1.77 \cdot 10^{-3}$
10.0	$\bar{N}$	*Al*	0	0	$4.1 \cdot 10^{-4}$
		Fe	0	0	$2.6 \cdot 10^{-4}$
		Pb	0	0	0
14.0	$\bar{N}$	*Al*	0	0	0
		Fe	0	0	0
		Pb	0	0	0
18.0	$\bar{N}$	*Al*	0	0	0
		Fe	0	0	0
		Pb	0	0	0

of electrons (positive ***and*** *negative) as functions of* t *and* $y_c =$

equal to $\bar{N}_s$ *(prim. phot. dep.).*

0	2	4	6	8	10
0.140	0.220	0.239	0.245	0.249	0.250
0.112	0.219	0.239	0.245	0.248	0.250
0.0594	0.218	0.238	0.244	0.247	0.249
0.243	0.400	0.456	0.483	0.502	0.522
0.195	0.396	0.451	0.478	0.497	0.517
0.103	0.391	0.445	0.471	0.491	0.510
0.314	0.580	0.701	0.781	0.847	0.912
0.251	0.569	0.688	0.766	0.832	0.897
0.133	0.556	0.669	0.746	0.812	0.877
0.356	0.757	0.985	1.14	1.30	1.46
0.285	0.736	0.959	1.11	1.27	1.43
0.151	0.710	0.925	1.07	1.23	1.39
0.373	0.942	1.30	1.61	1.91	2.24
0.298	0.905	1.25	1.55	1.85	2.18
0.186	0.858	1.19	1.48	1.78	2.10
0.237	1.81	3.49	5.79	8.6	12.2
0.190	1.68	3.27	5.48	8.21	11.7
0.158	1.51	3.00	5.07	7.69	11.0
0.130	2.52	6.35	13.6	25.0	43.1
0.104	2.30	5.88	12.7	23.6	40.9
0.0552	2.01	5.30	11.5	21.8	38.1
0.0392	2.20	11.8	40.1	104	242
0.0313	1.98	10.8	37.1	97	228
0.0166	1.71	9.65	33.6	88.3	210
$1.95 \cdot 10^{-3}$	0.412	9.2	76	387	1880
$1.56 \cdot 10^{-3}$	0.362	8.2	68	345	1750
$8.3 \cdot 10^{-4}$	0.292	6.93	58.1	305	1610
$1.8 \cdot 10^{-4}$	0.085	3.54	45	379	2980
$1.4 \cdot 10^{-4}$	0.075	3.08	40	339	2800
0	0.0618	2.56	32.8	285	2570
0	0.0111	0.83	15.7	186	2420
0	0.0094	0.72	13.8	169	2300
0	0.0073	0.59	11.5	149	2150

TABLE 3

l \ y_c			-3	-2	-1
24.0	$\bar{N}$	Al	0	0	0
		Fe	0	0	0
		Pb	0	0	0
29.0	$\bar{N}$	Al	0	0	0
		Fe	0	0	0
		Pb	0	0	0

TABLE 4. *Photon-initiated showers. The energy spectrum* $k_0 p(l, E)$ *for the secondary electrons (positive* **or** *negative) as a function of* l *and*

$$y = \log \frac{k_0}{E}.$$

l \ y	2	4	6	8	10
0.2	0.158	0.153	0.552	2.34	11.8
0.4	0.298	0.537	2.44	14.1	86.8
0.6	0.449	1.36	7.34	46.6	315
0.8	0.628	2.71	15.2	102	920
1.0	0.850	4.48	28.4	201	2030
2.0	2.30	21.6	207	1990	$1.92 \cdot 10^4$
3.0	3.56	48.7	624	7410	$8.82 \cdot 10^4$
5.0	2.89	108	2410	$4.14 \cdot 10^4$	$6.84 \cdot 10^5$
10.0	0.500	81.3	4700	$1.84 \cdot 10^5$	$7.11 \cdot 10^6$
14.0	0.0891	29.0	2580	$1.82 \cdot 10^5$	$1.26 \cdot 10^7$
18.0	0.0124	6.18	893	$9.44 \cdot 10^4$	$1.13 \cdot 10^7$
24.0	$5.83 \cdot 10^{-4}$	0.459	132	$2.29 \cdot 10^4$	$4.67 \cdot 10^6$
29.0	$4.41 \cdot 10^{-5}$	0.0404	22.8	$6.82 \cdot 10^3$	$1.78 \cdot 10^6$

TABLE 5. *Photon-initiated showers. The energy spectrum* $h(l, k)$ *for the* ***secondary*** *photons as a function of* l *and* $y_k = \log \frac{k_0}{k}$.

l \ y_k	2	4	6	8	10
0.2	0.0136	0.016	0.016	0.016	0.016
0.4	0.0483	0.0556	0.0588	0.0596	0.0607
0.6	0.0979	0.120	0.130	0.137	0.140

(continued).

0	2	4	6	8	10
0	$6.0 \cdot 10^{-4}$	0.071	2.34	44	947
0	$5.1 \cdot 10^{-4}$	0.060	2.04	39.7	901
0	$3.9 \cdot 10^{-4}$	0.048	1.67	34.5	843
0	$3.2 \cdot 10^{-5}$	0.0074	0.39	11.6	325
0	$2.5 \cdot 10^{-5}$	0.0062	0.33	10.6	312
0	$1.6 \cdot 10^{-5}$	0.0046	0.27	9.5	297

TABLE 5 *(continued).*

l \ y_k	2	4	6	8	10
0.8	0.158	0.193	0.225	0.240	0.262
1.0	0.224	0.299	0.350	0.389	0.450
2.0	0.535	0.923	1.40	2.00	3.06
3.0	0.768	2.09	4.23	6.92	11.6
5.0	0.776	4.32	13.4	31.6	83.1
10.0	0.170	3.85	28.2	132	728
14.0	0.0337	1.59	17.5	132	1210
18.0	$5.46 \cdot 10^{-3}$	0.385	6.44	66.8	1090
24.0	$2.99 \cdot 10^{-4}$	0.0363	0.966	14.1	438
29.0	$2.49 \cdot 10^{-5}$	$4.68 \cdot 10^{-3}$	0.156	3.39	150

TABLE 6. *Photon-initiated showers. The average number* $H_{sec}(l, y_c)$ *of secondary photons with energy above* E_c *as a function of* l *and* $y_c = \log \frac{k_0}{E_c}$. *The probability of finding the primary photon in the depth* l *is simply given by* $e^{-\alpha l}$, *which is given in the last column.*

l \ y_c	2	4	6	8	10	$e^{-\alpha l}$
1	0.25	0.78	1.4	2.2	3.0	0.55
5	0.64	4.7	21	61	170	0.050
10	0.12	2.7	28	150	840	$2.5 \cdot 10^{-3}$
14	0.025	0.92	14	120	1040	0
18	$3 \cdot 10^{-3}$	0.22	4.1	56	690	0
24	$3 \cdot 10^{-4}$	0.019	0.50	9.3	310	0
29	$3 \cdot 10^{-5}$	$2.7 \cdot 10^{-3}$	0.10	2.3	70	0

TABLE 7. *Electron-initiated showers. The energy spectrum* $h(l,k)$ *for the secondary photons as a function of* l *and* $y_k = \log \frac{E_0}{k}$.

l \ y_k	2	4	6	8	10	15
0.2	0.129	0.130	0.133	0.136	0.138	0.141
0.4	0.244	0.251	0.265	0.275	0.293	0.320
0.6	0.352	0.389	0.428	0.468	0.504	0.607
0.8	0.453	0.543	0.622	0.684	0.795	1.05
1.0	0.550	0.724	0.867	1.02	1.22	1.75
2.0	0.933	1.91	3.47	5.19	7.41	16.2
3.0	1.02	3.16	7.94	14.8	25.1	79.4
5.0	0.850	5.89	18.6	50.1	113	646
10.0	0.128	2.95	29.4	191	895	$1.79 \cdot 10^4$
14.0	0.0183	0.589	14.2	146	1250	$7.09 \cdot 10^4$
18.0	$2.44 \cdot 10^{-3}$	0.112	4.67	72.4	971	$1.39 \cdot 10^5$
24.0	$1.10 \cdot 10^{-4}$	$8.51 \cdot 10^{-3}$	0.603	17.0	333	$1.55 \cdot 10^5$
29.0	$8.5 \cdot 10^{-6}$	$7.9 \cdot 10^{-4}$	$8.5 \cdot 10^{-2}$	3.3	96	$9.1 \cdot 10^4$

TABLE 8. *Electron-initiated showers. The average number* $H(l,y_c)$ *of secondary photons with energy above* E_c *as a function of* l *and* $y_c = \log \frac{E_0}{E_c}$.

l \ y_c	2	4	6	8	10	15
1	0.83	2.0	3.7	5.5	7.8	15
5	0.50	5.2	26	91	250	1900
10	0.06	2.0	25	200	1200	$2.8 \cdot 10^4$
14	0.01	0.43	8.7	110	1200	$9.9 \cdot 10^4$
18	$1 \cdot 10^{-3}$	0.079	2.6	47	750	$1.7 \cdot 10^5$
24	$5 \cdot 10^{-5}$	$5.5 \cdot 10^{-3}$	0.31	9.1	220	$1.5 \cdot 10^5$
29	$4 \cdot 10^{-6}$	$5.9 \cdot 10^{-4}$	$6.3 \cdot 10^{-2}$	2.0	66	$6.8 \cdot 10^4$

Indleveret til Selskabet den 15. Marts 1940.
Færdig fra Trykkeriet den 14. Juni 1940.